Introduction to Magnetic Resonance

Principles and Applications

ROBERT T. SCHUMACHER
Carnegie-Mellon University

Modern Physics Monograph Series
EDITOR: FELIX VILLARS,
Massachusetts Institute of Technology
ROBERT T. SCHUMACHER,
Carnegie-Mellon University
Introduction to Magnetic Resonance:
Principles and Applications

W. A. *Benjamin, Inc. · New York, 1970*

INTRODUCTION TO MAGNETIC RESONANCE

Contents

CHAPTER 1

Basic Principles

Historically, experimental investigations into the quantum properties of angular momentum and magnetic moments followed the same course that now seems to be the most natural in introducing the subject conceptually. This first chapter is concerned with the concepts and the experiments on isolated atomic systems with angular momentum, which began with the molecular beam experiments of Stern in the 1920's and which lead naturally into the magnetic resonance experiments of Rabi in the 1930's. The material is probably familiar to all students with the background of an introductory course in modern physics. However, it is recommended that even students with confidence in their command of the subject study the chapter, if only to identify special terminology and points of view relied upon in later chapters. The student who finds the quantum mechanical references of Section 1-4 somewhat obscure should repair to the brief Appendix for some help, at least in the mathematical manipulations of the quantum mechanics of the spin $\frac{1}{2}$ system in magnetic fields.

1-1. DEFINITIONS

A system consisting of a mass undergoing circular motion about a fixed point in a plane has *angular momentum*. If the mass carries electrical charge, it has a *magnetic moment* that is proportional to the angular momentum. It is comforting to know that such simple statements are true in general for quantum mechanical systems, and that, for *magnetic dipole* moments, the proportionality factor is a scalar. The theorem stating this is an application of a powerful and ubiquitous statement known as the Wigner–Eckart theorem. We are concerned with angular momenta of various atomic, nuclear, and elementary particle systems. Table 1-1 shows the conventional symbols used for most of the systems in which we are interested. When the discussion is about an abstract angular momentum vector, we usually use the vector symbol **J**, which serves also as the total angular momentum of an atom.

Table 1-1
Conventional Symbols for Angular Momenta

System	Symbol
single electron spin	$\mathbf{S}$
electron orbit	$\mathbf{L}$
atom	$\mathbf{J} = (\mathbf{L} + \mathbf{S})$
nucleus	$\mathbf{I}$
atom including nucleus	$\mathbf{F} = \mathbf{I} + \mathbf{J}$

We also find it convenient to consider the angular momentum vector symbols to be dimensionless, and to display the units in which angular momentum is measured explicitly. The fundamental unit is, of course, $h/2\pi = \hbar$, Planck's constant. Thus, the Wigner–Eckart theorem states simply

$$\boldsymbol{\mu} = \gamma\hbar\mathbf{J} \tag{1-1}$$

where γ, the *gyromagnetic ratio* (more rationally, the magnetogyric ratio) is the scalar promised by the theorem. Now, if one pursues the example of the opening paragraph, the factor γ can be calculated immediately. The angular momentum is $|\hbar\mathbf{J}| = |\mathbf{r} \times m\mathbf{v}| = mr^2\omega$, where $\mathbf{r}$ is the orbit's radius, ω the angular frequency, m the mass, and $\mathbf{v}$ the velocity. The magnetic moment, in Gaussian units, is $\boldsymbol{\mu} = i\mathbf{A}/c$, where $A = \pi r^2$ is the orbit's area; the vector is perpendicular to the orbital plane, as in the case of the angular momentum. Thus,

$$\frac{iA}{c} = \frac{i\pi r^2}{c} = \frac{q\omega r^2}{2c} = \frac{J\hbar q}{2mc} \tag{1-2}$$

If the particle is an electron with charge $e = -4.8 \times 10^{-10}$ esu, and mass $m = 9.1 \times 10^{-28}$ g, the gyromagnetic ratio, $\gamma = e/2mc$, is related to the Bohr magneton:

$$\beta_0 = \frac{e\hbar}{2mc} = \hbar\gamma = -0.927 \times 10^{-20} \text{ ergs/G}$$

For nuclei, it is convenient to define a nuclear Bohr magneton

$$\mu_0 = \frac{|e|\hbar}{2Mc} = 5.05 \times 10^{-24} \text{ ergs/G}$$

where M is the proton mass.

Electrons, protons, neutrons, and μ mesons have intrinsic angular momentum. Atoms and nuclei of interest to us are compound systems, the total angular momentum and magnetic moment of which are still proportional by the Wigner–Eckart theorem, but the proportionality factor of which depends on the details of the system. Those details are conventionally absorbed into a *g factor*, or *spectroscopic splitting factor*. This factor is g_J, the Landé g factor for atoms, or $g = 2.000\ldots$, according to the Dirac equation, for electrons and μ mesons. We define the nuclear g factor by analogy. For the most part, it remains an experimental parameter characterizing nuclear moments, since, in most cases, nuclear theory is not yet able to provide better than rough estimates of its magnitude. In general, then, the expression

$$\boldsymbol{\mu}_J = g_J\left(\frac{e}{2mc}\right)\hbar\mathbf{J} = g\beta_0\mathbf{J} = \gamma_e\hbar\mathbf{J}$$

or

$$\boldsymbol{\mu}_I = g_I\mu_0\mathbf{I} = \gamma_n\hbar\mathbf{I} \tag{1-3}$$

gives the relation between $\boldsymbol{\mu}$ and $\mathbf{J}$, or $\mathbf{I}$, and it defines g. Equation (1-3) also defines the gyromagnetic ratio γ, which is now $g(e/2mc)$ for a system with intrinsic angular momentum (spin). Tables, particularly the most commonly encountered tables of nuclear moments, publish a quantity called "the magnetic moment in units of the Nuclear Bohr magneton." The maximum projection of $\mathbf{J}$ along any axis occurs for the state $M_J = J$. The magnetic moment is $\boldsymbol{\mu}_J = g\beta_0\mathbf{J}$, and the published number is gJ.

1-2. ENERGY IN AN EXTERNAL MAGNETIC FIELD: SPATIAL QUANTIZATION

The energy E of a magnetic moment μ in an external field[1] $\mathbf{H}$ is given by the familiar expression

$$E = -\boldsymbol{\mu} \cdot \mathbf{H} \tag{1-4}$$

or, in terms of the angular momentum,

$$E = -g\beta_0 H m_J \tag{1-5}$$

[1] In a vacuum it does not matter whether one uses H or B for the magnetic field if the quantities are expressed in Gaussian units. Strictly speaking, one should use B, but conventionally most of the literature uses H, a practice that we follow. Occasionally it is important to make the distinction in solid state physics applications, and then it is well established that the *correctly calculated* B is to be used.

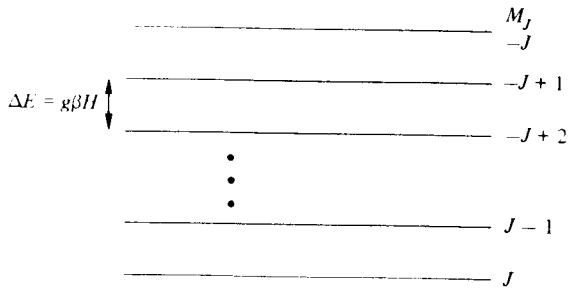

Fig. 1-1 Energy-level diagram for spin of angular momentum **J** in magnetic field **H**.

where m_J is the projection of **J** on **H**. Quantum mechanics restricts m_J to the $2J + 1$ integral or half-integral values. The energy-level diagram corresponding to Eq. (1-5) is shown in Fig. 1-1.

1-3. STERN–GERLACH EXPERIMENT

The application of a magnetic field H removes the $2J + 1$ degeneracy of the magnetic sublevels, as we have seen. Although these states are no longer degenerate, the energy differences between them are very small. In a field of 10^4 G, Eq. (1-5) corresponds to an energy separation of 1 cm^{-1} or about 10^{-4} eV for electron moments, 10^{-4} cm^{-1} or 10^{-8} eV for nuclear moments. This energy difference must be perceived against a background of 200 cm^{-1} or 0.025 eV of thermal energy at room temperature and several electron volts of energy for atomic transitions. Until the early 1920's, the consequences of spatial quantization had been manifested primarily through the Zeeman effect and the Faraday and other magneto-optic effects. The Zeeman effect was incompletely understood prior to the discovery of electron spin, and the quantitative relation of spatial quantization to the Faraday effect was obscure.

The reality of spatial quantization was demonstrated in a particularly graphic fashion by the Stern–Gerlach experiment, successfully performed in 1922. If a beam of neutral atoms passes through a homogeneous magnetic field, it is undeflected by that field, even though the magnetic degeneracy is lifted. But if the field is not spatially homogeneous, there is a net force on the moments in the beam that is given by the expression

$$\mathbf{F} = (\boldsymbol{\mu} \cdot \nabla)\mathbf{H} = \mu_x \frac{\partial \mathbf{H}}{\partial x} + \mu_y \frac{\partial \mathbf{H}}{\partial y} + \mu_z \frac{\partial \mathbf{H}}{\partial z} \qquad (1\text{-}6)$$

There is a component of this force that is constant while the moment is in the gradient, and it produces a deflection of the beam that is proportional to μ_z. To see that, choose the following simplest possible field gradient. See Fig. 1-2. The beam travels in the x direction with the

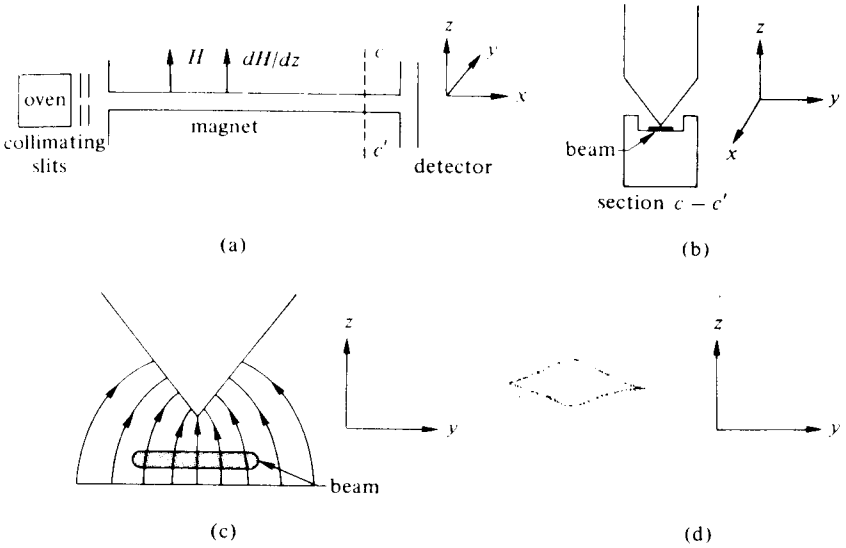

Fig. 1-2 Schematic representation of Stern–Gerlach apparatus. (a) Arrangement of main components: oven, collimating slits, magnet, and detector. (b) Cross section $c - c'$ of (a). (c) Enlarged view of beam and magnetic field in region of the beam. (d) Appearance of film deposited on substrate in original experiments of Stern.

field arranged so that $H_x = 0$. The field is principally in the z direction. All derivatives of H with respect to x vanish, and, in the beam region, both $\nabla \cdot \mathbf{H} = 0$ and $\nabla \times \mathbf{H} = 0$ are satisfied. The components of Eq. (1-6) are

$$F_x = 0 \qquad F_y = \mu_y \frac{\partial H_y}{\partial y} + \mu_z \frac{\partial H_y}{\partial z} \qquad F_z = \mu_y \frac{\partial H_z}{\partial y} + \mu_z \frac{\partial H_z}{\partial z} \qquad (1\text{-}7)$$

Furthermore, let the beam lie in the symmetry plane $y = 0$, where $H_y = 0$ (Fig. 1-2c). Then $\partial H_y/\partial z = 0$, and, since $\nabla \times \mathbf{H} = 0$, $\partial H_z/\partial y = \partial H_y/\partial z = 0$. Since $\nabla \cdot \mathbf{H} = 0$, $\partial H_y/\partial y = -\partial H_z/\partial z$, Eq. (1-7) reduces to

$$F_x = 0 \qquad F_y = -\mu_y \frac{\partial H_z}{\partial z} \qquad F_z = \mu_z \frac{\partial H_z}{\partial z} \qquad (1\text{-}8)$$

In the next section, we emphasize in great detail that the magnitude of the field H_z produces a torque $\boldsymbol{\mu} \times \mathbf{H}$, causing a precession about $\mathbf{H}$ (which is virtually entirely H_z at the beam coordinate) such that μ_z is constant and μ_y oscillates about an average value of zero. So the only component of the force that produces a net deflection is in the z direction, and it may be written in terms of the magnetic quantum number as $F_z = m_J g \beta_0 (\partial H_z/\partial z)$. The presence of m_J means that the beam splits into $2J + 1$ components. The first experiment was done on silver (partly because the deposit could be easily "developed"), and two components were seen, as illustrated in Fig. 1-2d.[2] We now know that $2J + 1 = 2$ requires $J = \frac{1}{2}$, and that the ground state of the silver atom is an orbital S state with a single electron of spin $\frac{1}{2}$. The first experiment was done prior to the discovery of electron spin, but the result was not interpreted as requiring half-integral spin since it was assumed silver had an orbital angular momentum $L = 1$ and the $m_L = 0$ state was not allowed in old quantum theory.

Even in its simplest form the experiment has several components, none trivial, so that molecular beam experiments have long been known as the most difficult in atomic physics. The experimental problems to be solved include a high enough vacuum so that a typical beam atom can traverse the apparatus without colliding with a residual gas molecule in a meter or more of flight. The source, usually an oven with a small hole, must produce a well-collimated beam. The field gradient must be as large as possible, but the magnetic field itself cannot change too abruptly in time as sensed by the moving magnetic moment that passes from the fieldfree region to a region of maximum field gradient, and then out again to a fieldfree region before striking the detector. Finally, some device must detect, with considerable spatial resolution, the beam intensity. The modern solution of these problems is discussed in detail in the definitive monograph on molecular beams by Ramsey [2]. A somewhat briefer discussion appears in another standard reference in the field of magnetic resonance, Kopfermann's *Nuclear Moments* [3]. Among the refinements particularly useful when two Stern–Gerlach apparatuses are put in series for the standard molecular beam resonance experiment (Section 1-4) have been velocity selectors between the oven and the field region so all molecules in the beam receive the same deflection. Sophisticated universal detectors, which partially ionize the beam and send it through a simple mass spectrometer before it registers on the ultimate detector, have also

[2] The student will find it an amusing exercise in the propagation of errors to watch for illustrations such as Fig. 1-2 in which the beam is traveling in the y direction, transverse to the long dimension of the apparatus. As far as I can determine, the first such incorrect illustration appeared in A. Sommerfeld's *Atombau und Spectrallinien* [1], in all editions subsequent to 1923. It is reproduced in many texts of that school, but it also still appears in texts published in the United States as recently as 1967.

been developed. (See references listed at the end of the chapter for more discussion of experimental techniques.)

The Stern–Gerlach technique, by itself, reached its pinnacle of usefulness under the direction of Stern, particularly with the aid of Otto Frisch and I. Estermann. Although the resonance method of Rabi did prove to offer unheard of precision compared to the nonresonant experiments, the basic technique did provide a few triumphs beyond the first demonstration of spatial quantization. One of these was the discovery of the anomalous g factor of the proton (i.e., that $g_p = 5.59\ldots$ rather than $g = 2.000\ldots$, as expected from the Dirac theory of a spin $\frac{1}{2}$ particle). The initial report of this work appeared in *Nature* in 1933 [4], and it is a model of elegant brevity. The student who understands it, sentence by sentence, has a good working grasp of many of the necessary fundamentals of modern physics.

It should be emphasized that the Stern–Gerlach apparatus is a very useful practical example of a quantum mechanical state selector, or beam polarizer. The separated beams of moments of that energy from the field gradient region, each characterized by its own m_J, are polarized. The apparatus may be reversed in function and a partially or fully polarized beam sent in. Its trajectory in the apparatus is determined by the state function (i.e., the m_J level) of the constituents of the beam, so the apparatus now functions as an analyzer. These functions are important to understand and distinguish in following the magnetic resonance experiment of Rabi. A comprehensive discussion is given in volume 3 of the *Feynman Lectures on Physics* [5].

1-4. THE RABI MAGNETIC RESONANCE EXPERIMENT

If a Stern–Gerlach apparatus can be a state selector, it can also be an analyzer. What could be more natural than to put two of them in series, with some experiment in between? In the 1930's, Rabi, who had done postdoctoral work under Stern at Hamburg, performed the first magnetic resonance experiment and made the first precision nuclear magnetic moment measurement, in a homogeneous magnetic field between a polarizer and analyzer. Figure 1-3 shows two inhomogeneous fields, produced by the conventionally designated A and B magnets, with the homogeneous C magnet between them. In the C region, the magnetic resonance experiment causes transitions between magnetic quantum levels. Consider a $J = \frac{1}{2}$ system. Figure 1-3 shows the polarizer and analyzer with field gradients in the same direction. Also, care is taken that the direction of the field H itself always points in the same direction. At the end of the polarizer, one of the two separated beams may be deflected or stopped by a baffle, leaving a beam of pure $m_J = \frac{1}{2}$ particles, for instance,

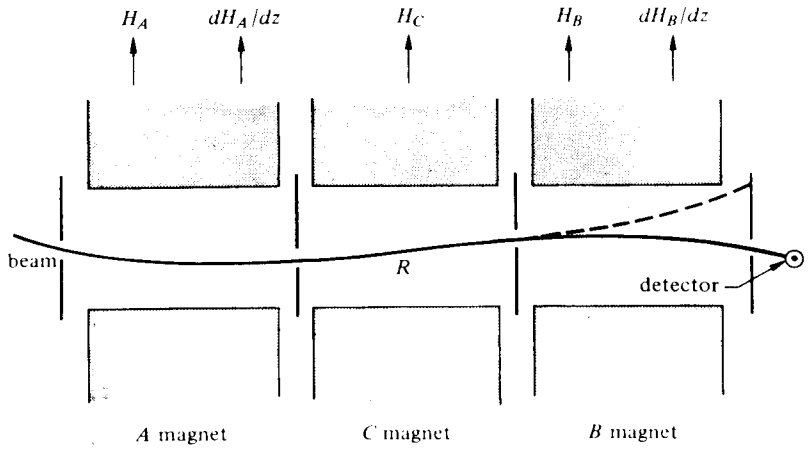

Fig. 1-3 Fields and beam trajectories in Rabi resonance experiment. The solid curved line is a greatly exaggerated trajectory for a spin $\frac{1}{2}$ system that undergoes a transition from $m_J = \frac{1}{2}$ to $m_J = -\frac{1}{2}$ in the resonance region R in the homogeneous C magnet. The dotted line in the B magnet represents the path of a molecule that does not undergo a transition and is prevented by the baffle from reaching the detector.

to enter the C magnet. If nothing is done to them there, they enter the second Stern–Gerlach apparatus where they are further deflected. If the detector is placed to detect a beam that comes through undeviated, it will detect no signal. If the beam in the C region is manipulated so that some or all of the moments are put into the $m_J = -\frac{1}{2}$ state, then in the B field their deflection will be down, and, if the A and B magnets are identical, then the B magnet will reverse the deflection produced by the A magnet, and the beam will hit the detector.

Some of the preceding details are arbitrary and of no particular importance. The experiment as described is known in the molecular beam trade as a "flop-in" experiment: the change of state in the C region causes the beam to "flop-in" to the detector. A different position of the detector, or reversal of the gradient in the B region, could result in a "flop-out" experiment. What is not unimportant is the maintenance of a magnetic field oriented in the same direction through the apparatus, or, if the field does reorient, it must do so slowly, as seen by the moment as it moves through the various regions. The first restriction is required so that the beam remains in the same quantum mechanical state unless a transition to another state is deliberately produced in the C region. The second restriction is required so that no "accidental" transitions occur between magnets.

We turn now to the theory of the magnetic resonance experiment. The quantum mechanical and classical equations of motion of a spin in a magnetic field are identical: the latter equations are for classical angular momenta and magnetic moments; the former are for expectation values of angular momentum operators. It is often sufficient to consider only the classical case. Figure 1-4 shows an angular momentum $\mathbf{J}$, moment $\boldsymbol{\mu}$,

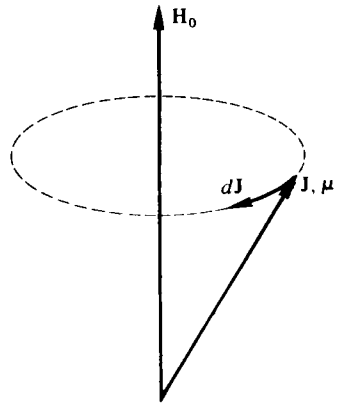

Fig. 1-4 Magnetic moment $\boldsymbol{\mu} = \gamma\hbar\mathbf{J}$ precessing in a constant field $\mathbf{H}_0$. The figure is drawn for positive γ.

inclined at an arbitrary angle with respect to the z axis, the field direction. The classical equation of motion is

$$\hbar \frac{d\mathbf{J}}{dt} = \boldsymbol{\mu} \times \mathbf{H}_0 = \gamma\hbar\mathbf{J} \times \mathbf{H}_0 \tag{1-9}$$

The change in $\mathbf{J}$ during dt, $d\mathbf{J} = \gamma\hbar\mathbf{J} \times \mathbf{H}_0\, dt$, is perpendicular to the plane defined by the vectors $\mathbf{J}$ and $\mathbf{H}_0$. The motion is a precession, with $\mathbf{J}$ defining a cone with the axis $\mathbf{H}_0$. The angle between $\mathbf{J}$ and $\mathbf{H}_0$ remains constant. The precession frequency, $\omega_0 = \gamma H_0$, is known as the Larmor frequency.

In the molecular beam resonance method, H_0 is a spatially homogeneous field produced by the C magnet. In addition, a transverse alternating field $H_1(t)$ is applied at frequency ω in the C magnet region.

$$\mathbf{H}_1(t) = 2\mathbf{i}H_1 \cos \omega t \tag{1-10}$$

In the presence of the alternating field, the equation of motion is

$$\frac{d\mathbf{J}}{dt} = \gamma\mathbf{J} \times (\mathbf{k}H_0 + \mathbf{i}2H_1 \cos \omega t) \tag{1-11}$$

The problem is to find $\mathbf{J}(t)$. Approximate solution to (1-11) can be obtained easily by transforming to an appropriate rotating coordinate system. There is a theorem, proven in all classical mechanics courses, to the effect that the time derivative of $\mathbf{J}$ as viewed from a rotating coordinate system, $\partial\mathbf{J}/\partial t$, is related to $d\mathbf{J}/dt$, the time derivative as viewed from a stationary coordinate system, by the expression

$$\frac{d\mathbf{J}}{dt} = \frac{\partial \mathbf{J}}{\partial t} + \boldsymbol{\omega} \times \mathbf{J} \tag{1-12}$$

where $\boldsymbol{\omega}$ is a vector whose magnitude gives the angular frequency of rotation of the rotating system and whose direction is the axis about which the system rotates. Some necessary insight is obtained by substituting (1-12) into (1-9):

$$\frac{\partial \mathbf{J}}{\partial t} + \boldsymbol{\omega} \times \mathbf{J} = \gamma \mathbf{J} \times \mathbf{H}_0$$

or (1-13)

$$\frac{\partial \mathbf{J}}{\partial t} = \gamma \mathbf{J} \times \left(\mathbf{H}_0 + \frac{\boldsymbol{\omega}}{\gamma}\right)$$

That is, as far as the rate of change of $\mathbf{J}$ is concerned, transforming to a rotating reference system at $\boldsymbol{\omega}$ is the same as adding an effective field $\boldsymbol{\omega}/\gamma$, and considering the motion in the effective field

$$\mathbf{H}_{\text{eff}} = \mathbf{H}_0 + \frac{\boldsymbol{\omega}}{\gamma} \tag{1-14}$$

It follows immediately that $\mathbf{J}$ is time independent in a rotating coordinate system such that $\mathbf{H}_{\text{eff}} = 0$, or $\boldsymbol{\omega} = -\gamma\mathbf{H}_0$. The result, and the transformation, are intuitive for this case. The sense of rotation of $\mathbf{J}$, as seen in the laboratory (i.e., stationary) frame in Fig. 1-4, is just the sense of rotation of the rotating coordinate system necessary to "stop" the motion.

The solution of the problem with alternating (or, conventionally, radio frequency or rf) field, Eq. (1-11), can be obtained from the rotating coordinate transformation after observing the following: decompose $H_1(t)$ into two circularly polarized components of equal amplitude rotating in opposite directions in the xy plane.

$$\mathbf{H}_1(t) = \mathbf{H}_a + \mathbf{H}_b \tag{1-15}$$

where

$$\mathbf{H}_a = H_1(\mathbf{i}\cos\omega t + \mathbf{j}\sin\omega t)$$

and

$$\mathbf{H}_b = H_1(\mathbf{i}\cos\omega t - \mathbf{j}\sin\omega t) \tag{1-16}$$

Simple inspection shows that $\mathbf{H}_b$ is rotating in the same sense as the moment in Fig. 1-4, and $\mathbf{H}_a$ in the opposite sense. A rotating coordinate transformation to a system defined by $\boldsymbol{\omega} = \mathbf{k}\omega$ leaves the field H_b stationary in the transformed system, but the component rotating in the opposite sense rotates at 2ω in the rotating coordinate system. To see that we may neglect $\mathbf{H}_a$ under most circumstances, examine the effect of $\mathbf{H}_b$ alone. Figure 1-5 shows the fields $\mathbf{H}_0$ and $\mathbf{H}_b$ as they appear in the rotating system

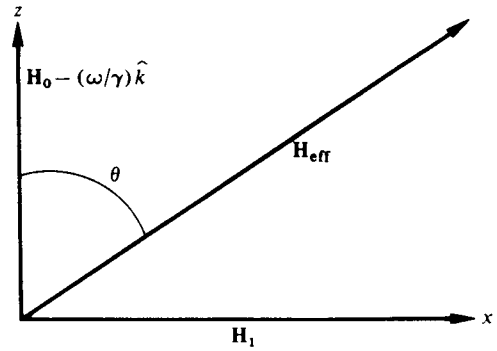

Fig. 1-5 Fields and angles in the coordinate system rotating at $\boldsymbol{\omega} = -\mathbf{k}\omega$.

in which $\mathbf{H}_b$ appears stationary, that is, the rotating system defined by the transformation $\boldsymbol{\omega} = -\mathbf{k}\omega$.

The effective field in the z direction is $\mathbf{k}(H_0 - \omega/\gamma)$ from Eq. (1-14). The total effective field is given by

$$\mathbf{H}_{\text{eff}} = \mathbf{k}\left(\mathbf{H}_0 - \frac{\omega}{\gamma}\right) + \mathbf{i}\mathbf{H}_1 \tag{1-17}$$

The angle θ is defined by

$$\tan\theta = \frac{H_1}{H_0 - \omega/\gamma} \tag{1-18}$$

The motion of a magnetic moment initially along the z direction consists, in the rotating system, of precession about $\mathbf{H}_{\text{eff}}$ with an angular frequency $\omega_{\text{eff}} = \gamma H_{\text{eff}}$ with the angle θ constant. That is, the vector $\boldsymbol{\mu}$ precesses on the surface of a cone having angle θ and axis $\mathbf{H}_{\text{eff}}$.

A brief digression from the main line of the development is necessary to dispose of the counterrotating component $\mathbf{H}_a$. The fields we have considered produce their effect by virtue of being static in the rotating frame. $\mathbf{H}_a$ rotates at 2ω in that frame, which means that whereas it acts to produce the same general effect as $\mathbf{H}_b$ when it is approximately parallel to it, it produces the opposite effect at a time $\pi/2\omega$ later, when it is directed opposite to $\mathbf{H}_b$. On the average, we expect its effect to be zero. This result has several consequences. First, it is only necessary to apply a linearly polarized rf field in the C region, for we shall be certain, regardless of the algebraic sign of γ, that one of the rotating components will produce some precession of the moment away from the z direction. We arbitrarily chose the magnitude of the linearly polarized field to be $2H_1$, so that the rotating component's amplitude would be the conventional H_1. We could have applied a circularly polarized rf field, and that procedure is the one commonly used to determine the sign of γ.

The arguments we have used to dispose of the counterrotating component were qualitative ones. Quantitatively, the neglect of the counterrotating component is valid only if $(H_1/H_0) \ll 1$. Experiments have been done in fields for which this inequality is not well obeyed. The result is a shift in the radio frequency that produces the maximum effect in tipping the moment to the $-z$ direction. It goes by the name "Bloch–Siegert shift."

For future work, it is important to notice here the obvious fact that as the moment begins to precess around $\mathbf{H}_{\text{eff}}$, it acquires a component in the xy plane. In the laboratory frame, that component is rotating at the angular frequency ω. To make the connection with the magnetic resonance experiment done in the C-field region, between two Stern–Gerlach apparatuses, we must discuss transitions between m_J states, something the preceding discussion of a classical moment seemingly contains no hint of. Let us specialize the discussion to the case of a spin $\frac{1}{2}$ system. The orientation of the classical moment along the z direction is related to the probability that the spin is in the $+\frac{1}{2}$ or $-\frac{1}{2}$ m_J state. If the spin wave function is $|\chi\rangle = a|\tfrac{1}{2}\rangle + b|-\tfrac{1}{2}\rangle$, then $P(\frac{1}{2})$, the probability the spin is in the $|\frac{1}{2}\rangle$ state, is $|\langle\frac{1}{2}|\chi\rangle|^2 = |a|^2$ and $P(-\frac{1}{2}) = |\langle -\frac{1}{2}|\chi\rangle|^2 = |b|^2$. We consider the function,

$$\cos\alpha = |a|^2 - |b|^2 \qquad 0 < \alpha < \pi \tag{1-19}$$

with the subsidiary normalizing condition that $|a|^2 + |b|^2 = 1$ (there is certainty of finding the spin in one or the other of the states). The function

$\cos\alpha$ has, in fact, the properties of the projection of the spin on the z axis, and it is through $\cos\alpha$ that we make the connection to the classical calculation. Again, defining $\cos\alpha = \boldsymbol{\mu}\cdot\mathbf{H}_0/|\mu|\,|H_0|$, we find, after some three-dimensional geometry,

$$\cos\alpha = 1 - 2\sin^2\theta\sin^2\frac{\gamma H_{\text{eff}}\,t}{2} \tag{1-20}$$

where we assumed the boundary condition $\alpha = 0$ at $t = 0$. Using the normalizing condition $|a|^2 + |b|^2 = 1$, we can also write (1-19) as

$$\cos\alpha = 1 - 2|b|^2 \tag{1-21}$$

Comparison of (1-20) and (1-21) yields immediately

$$P(-\tfrac{1}{2}) \equiv |b|^2 = \sin^2\theta\sin^2\frac{\gamma H_{\text{eff}}\,t}{2} \tag{1-22}$$

for the probability that, at time t, the spin is in the state $m_J = -\frac{1}{2}$, having started in state $m_J = \frac{1}{2}$ at $t = 0$.

Equation (1-22) checks the result obtained by inspection of Fig. 1-4; namely, that for $\theta = 90°$, the spin precesses to the $-z$ direction in a time $t = \pi/\omega_{\text{eff}} = \pi/\gamma H_{\text{eff}}$. Of course, $\theta = 90°$ corresponds to the condition of exact resonance,

$$\omega = \omega_0 = \gamma H_0 \tag{1-23}$$

It is clear from (1-21) and (1-22) that the probability of a spin being in either of the $m_J = \pm\frac{1}{2}$ states varies periodically, with a full cycle completed with angular frequency γH_{eff}. What is less clear, since we have not done a full quantum mechanical treatment but have only made a plausible connection to quantum mechanics, is that the amplitudes $a(t)$ and $b(t)$ of the $m_J = +\frac{1}{2}$ and $m_J = -\frac{1}{2}$ states, respectively, vary in time in a coherent fashion. The significance of that statement is that the transverse components of angular momentum operators, J_x and J_y, have nonzero but time dependent values. For our future discussion of transient methods in magnetic resonance, as well as the discussion of the Ramsey modification of the molecular beam resonance method, it is most interesting to imagine doing the experiment at exact resonance ($\sin\theta = 1$), and turning off H_1 when $\omega_{\text{eff}} t = \pi/2$. Then $P(\frac{1}{2}) = P(-\frac{1}{2}) = \frac{1}{2}$. In the rotating frame, the amplitudes a and b are constant and equal in magnitude (but, since they

are complex, not necessarily equal in phase). We can write the spin wave function $|\chi\rangle$ to be $|\chi\rangle = (2)^{-1/2}\,[|\tfrac{1}{2}\rangle + e^{+i\phi}\,|-\tfrac{1}{2}\rangle]$. The expectation value of J_x is, if we suppress the time dependence from the Larmor precession,

$$\begin{aligned}\langle J_x\rangle &= \tfrac{1}{2}[\langle\tfrac{1}{2}| + e^{-i\phi}\,\langle-\tfrac{1}{2}|]J_x[|\tfrac{1}{2}\rangle + e^{i\phi}\,|-\tfrac{1}{2}\rangle] \\ &= \tfrac{1}{2}[\langle\tfrac{1}{2}|J_x|-\tfrac{1}{2}\rangle e^{i\phi} + \langle-\tfrac{1}{2}|J_x|\tfrac{1}{2}\rangle\, e^{-i\phi}] \qquad (1\text{-}24) \\ &= \frac{\cos\phi}{2}\end{aligned}$$

where ϕ is the phase difference between a and b. It would, in fact, be zero for the example we have used. The important point is that, just as in the classical case, the angular momentum has been turned over toward the xy plane. Viewed in the laboratory frame, it is precessing at ω_0, and will continue to do so indefinitely *with the same phase* as long as nothing perturbs it. The point to emphasize is that the transverse components of **J**, J_x and J_y, arise from coherent linear superpositions of state functions of the various m_J states. Later, when we deal with ensembles of spins, the question of the relative coherence of the superposition from one spin to the next will be crucial.

The Rabi molecular beam magnetic resonance experiment is done by applying a transverse rf magnetic field in the C magnet. The original, and still common, method of applying the rf field is by means of the "hairpin," shown in Fig. 1-6. The intensity of the beam at the detector is monitored as a function of the radio frequency ω. A typical intensity $I(\omega)$ versus frequency curve has the bell-shaped appearance of Fig. 1-7,

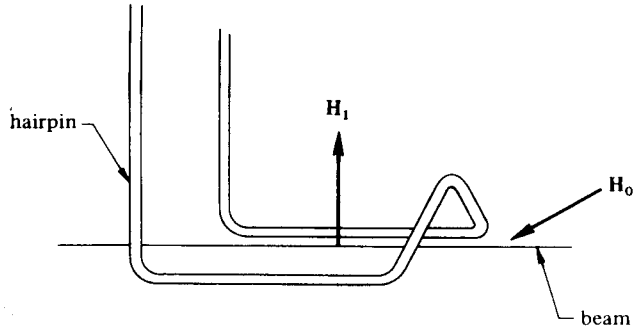

Fig. 1-6 The "hairpin," a method of applying the rf field in the C magnet of a resonance experiment.

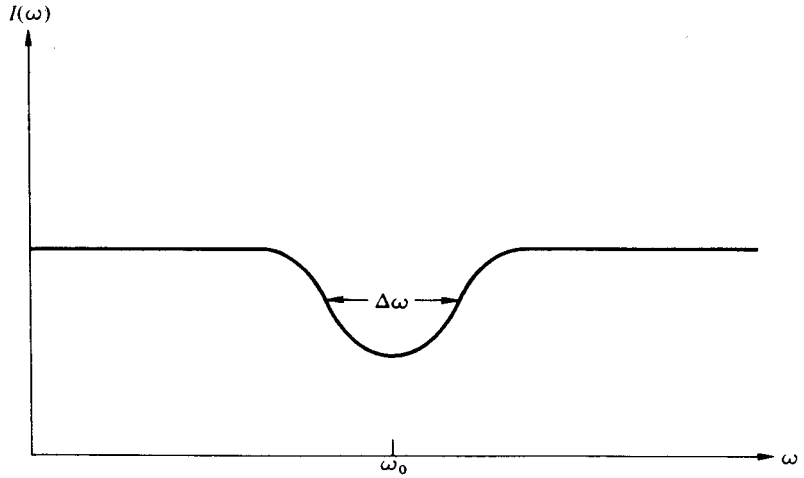

Fig. 1-7 Beam intensity at the detector as a function of the frequency of the rf field in the C magnet.

which has been drawn for a hypothetical "flop-out" experiment. The exact shape of the curve is of no particular interest to us, but there is something to be learned by examining the origins of its width, $\Delta\omega$. Since the first object of a beam resonance experiment is to find ω_0, it is important to make $\Delta\omega$ as small as possible. Experimentalists sometimes use the rule of thumb that the frequency ω_0 can be located to within $\Delta\omega$ divided by the signal-to-noise ratio. (Of course, we showed no noise in Fig. 1-7, but it is inevitably there in experimental data.) In the natural effort to make the signal as large as possible, to obtain the optimum "flop-out," the experimenter adjusts the magnitude of H_1 so that, in language appropriate to a $J = \frac{1}{2}$ system, the opposite spin state has the largest possible amplitude at $\omega = \omega_0$. From Eq. (1-22), that occurs when $\gamma H_1 t = \pi$. The time t here is the time of flight of the moment through the hairpin. Approximately half the amplitude of the signal occurs when ω is such that $P(\frac{1}{2}) = P(-\frac{1}{2}) = \frac{1}{2}$. We assume t and H_1 are fixed by the criterion $H_1 t = \pi/\gamma$. Then the half-maximum intensity occurs for $\cos\alpha = 0$ in Eqs. (1-20) or (1-21), or $P(-\frac{1}{2}) = |b|^2 = \frac{1}{2}$ in (1-22). We leave it as an exercise for the reader—an exercise involving primarily the solution of a transcendental equation—to show that $P(\frac{1}{2}) = P(-\frac{1}{2}) = \frac{1}{2}$ when $H_{\text{eff}} = 1.275H_1$, or $\theta = 51.5°$, and $(H_0 - \omega/\gamma) = 0.8H_1$. It follows that the full width at half-maximum intensity, the $\Delta\omega$ of Fig. 1-7, is $\Delta\omega = 1.6\gamma H_1$. When it is coupled with the other requirement, which we have expressed as $\gamma H_1 t = \pi$, we obtain

$$\Delta\omega t = 1.6\pi \qquad (1\text{-}25)$$

Equation (1-25) looks very much like the uncertainty principle, which relates the precision with which the energy may be established to the time over which the measurement is made. That is exactly what Eq. (1-25) is, for t is the time during which the system is in the probing field H_1. Correct use of the uncertainty principle argument would have obviated the somewhat tedious calculation of the line width, but the effort was worthwhile since it was instructive.

To achieve greater precision, the experimenter must increase t, the time in the apparatus. That goal can be accomplished by selecting the slowest molecules coming from the oven—but with the certain result of a loss in intensity—and also by increasing the length in the beam direction of the C-field magnet and the hairpin. The limitation in $\Delta\omega$, soon reached, is not from the preceding considerations, but rather from the inhomogeneity of the C field. The larger the magnet the harder it is to produce one with a homogeneity of field that is less than the natural limitations of Eq. (1-25). To overcome this limitation, Ramsey devised a very beautiful technique, which we examine briefly for its own sake and for what it can contribute to the understanding of later magnetic resonance experiments.

Consider a monochromatic beam (i.e., constant velocity v) so that each molecule in the beam spends the same time in the hairpin. Ramsey split the hairpin into two parts, both driven by an rf oscillator such that the phase of the rf field is the same in each. They are both in the C magnet, but situated at opposite extremities of the homogeneous field. Figure 1-8

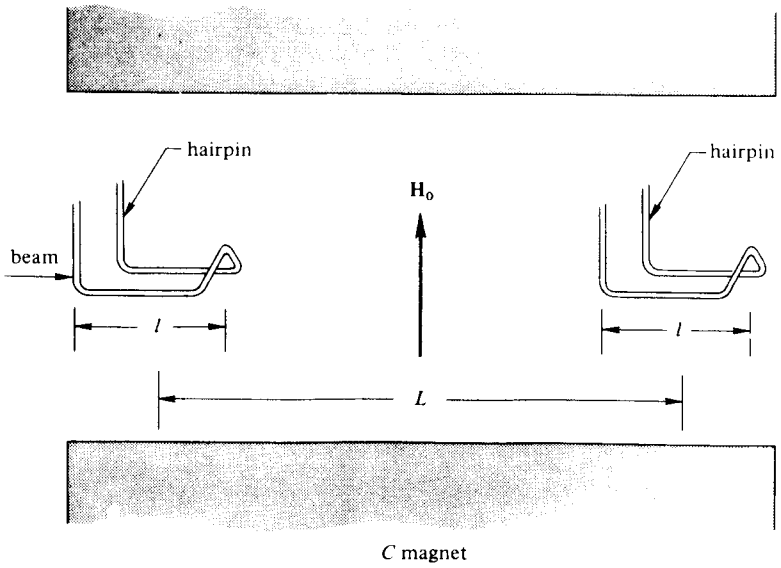

Fig. 1-8 Ramsey split rf field experiment.

shows the arrangement and defines some of the quantities we need. The length L is much greater than l. The latter is adjusted so that $\gamma H_1 t_l = \pi/2$, where $t_l = l/v$. If the beam enters the hairpin in the $m_J = \frac{1}{2}$ state, it leaves in an equal admixture of $m_J = \frac{1}{2}$ and $-\frac{1}{2}$ states, with phase coherence in the admixture. That is, the angular momentum is in the transverse plane and precesses freely about H_0 at $\omega = \gamma H_0$. In the time $t_L = L/v$ it takes for the beam to reach the other hairpin, it precesses an angle Φ in the xy plane. We define the average field $\bar{H}_0$ and the average frequency $\bar{\omega}_0$ by the relation

$$\Phi = \bar{\omega}_0 t_L = \gamma \bar{H}_0 t_L \tag{1-26}$$

The average $\bar{H}_0$ is a spatial average of the fields that the beam sees. (We have assumed for simplicity that the beam has zero transverse dimensions, so that each moment in the beam samples the same H_0.) Adjust the frequency of the oscillator driving the hairpins to be exactly ω_0. Then the rf phase of H_1 at the second hairpin is the same as the phase of the transverse component of $\mathbf{J}$; that is, they have the same spatial orientation, so that in the frame rotating at ω_0 the moment continues the precession from the $+z$ to the $-z$ direction that it started in the first hairpin.

Figure 1-9 illustrates the precessions schematically in the rotating reference system. The extent of the improvement of this technique over the single rf field region method can be estimated by the appropriate uncertainty principle argument. The line width $\Delta\omega_{\text{Ramsey}}$ would have to obey

$$\Delta\omega_{\text{Ramsey}}\ t_L \simeq 2\pi \tag{1-27}$$

by analogy with (1-25). Hence, $\Delta\omega_{\text{Ramsey}}/\Delta\omega_{\text{conventional}} \sim t_l/t_L \sim l/L$. To see that t_L is indeed the appropriate "measurement time" to insert in an uncertainty principle argument, examine what happens when the radio frequency is not quite ω_0, but is $\omega_0 + \Delta\omega_R$. We now define $\Delta\omega_R$ precisely by noting, as suggested in Fig. 1-9b, that if, during the time t_l, the rf oscillator accumulates phase $\Phi \pm \pi$, then the $\mathbf{H}_1$ seen by the spins in the second hairpin is in the $-y$ direction in the frame rotating at ω_0. The precession of the spins about that field undoes the work of the first hairpin, so the spins precess up to the $+z$ direction again. If precession to the $-z$ direction gives a maximum at the detector, then this second case corresponds to an absolute minimum in the signal. The rf oscillator frequency corresponding to this minimum signal is just

$$(\bar{\omega}_0 + \Delta\omega_R)t_L = \Phi \pm \pi \tag{1-28}$$

or

$$\Delta\omega_R = \pm\pi/t_L$$

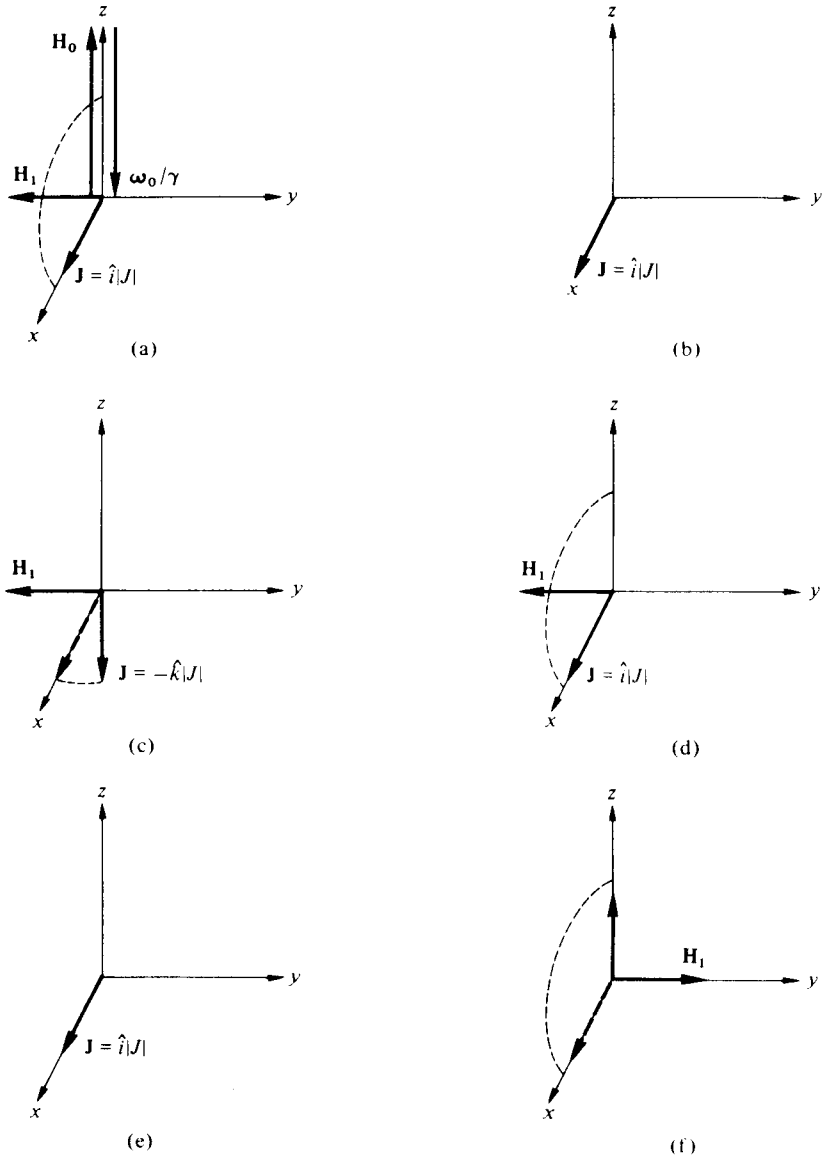

Fig. 1-9 Rotating frame precession of the magnetic moment in the Ramsey split rf field experiment. (a) Precession in the first hairpin. (b) Average orientation of **J** between hairpins. (c) Motion in second hairpin. (d), (e), and (f) Same as (a), (b), and (c) except for reversal of rf phase at second hairpin. See text.

The full width between the minima is $\Delta\omega_R = \pm 2\pi/t_L$. Although $\Delta\omega_R$ calculated this way is almost the same as the "blind" extension of (1-25), not too much should be made of the fact since different quantities are being calculated, which depend in detail on the shape of the resonance line. The shape of a Ramsey curve for a "flop-in" experiment is shown in Fig. 1-10. The width $\Delta\omega$ is roughly the width obtained if the split rf fields are put together.

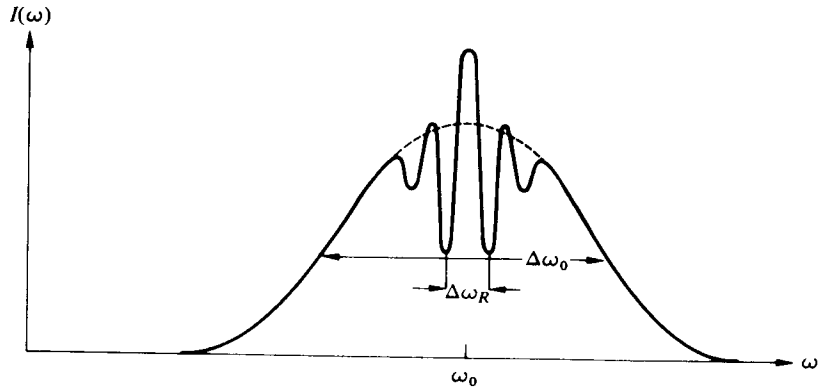

Fig. 1-10 Detector intensity as a function of frequency for the Ramsey experiment.

1-5. APPLICATIONS AND LITERATURE SURVEY

For precision measurements of magnetic moments, the simple Stern–Gerlach apparatus was almost totally eclipsed by resonance methods. The molecular beam techniques by themselves have been used, however, in some important investigations. One of the most obvious is the investigation of the velocity distribution of the beam emitted from the hole of an oven at temperature T. The last publication by Stern before his retirement was an investigation of this subject, which, incidentally, was the topic that prompted his interest in molecular beams in the first place. In the paper by Estermann *et al.* [6], the analysis of the velocities of the molecules is done by measuring their *fall*, or downward deflection, in the earth's *gravitational* field! One rarely encounters any practical consequence of an atomic particle's *gravitational* mass in laboratory atomic physics.

The combined Stern–Gerlach and magnetic resonance experiments of Rabi gave the first precise measurements of nuclear moments, and they are still used for this purpose, particularly, in recent years, to measure

nuclear moments of radioactive nuclei. The number of applications is so large as to defy even reasonable enumeration. The student would be advised to read the elementary review articles of Frisch [7] and of Kusch [8], as well as to look into some of the comprehensive tomes, such as Ramsey [1]. Reading the original literature in this field provides a palatable introduction to scientific literature in journal form. Much of it appeared in the 1930's, when brevity to the point of total obscurity was not yet the hallmark of most papers in contemporary journals. The first comprehensive discussion by Rabi *et al.* [9] of the molecular beam, magnetic resonance method, and the first measurement of the anomalous moment of the electron [10] both are relatively readable by upper-division students with vector-model type command of atomic physics. Some further applications of particular importance will be discussed in Chapter 6.

I cannot resist concluding this chapter by remarking on the central position occupied by the Stern–Gerlach experiment in modern quantum physics. The reason seems not to be any particular uniqueness or profundity of the technique, but rather the simplicity of the technique as an example of the problem of state preparation in quantum mechanics. It serves not only as a favorite pedagogical vehicle (see Feynman, vol. 3 [5]) but also as a source of "*gedanken* experiments" for weighty discussion of such vexing questions as the problem of measurement in quantum mechanics. For an example of the latter, see Wigner, *Symmetries and Reflections* [11], particularly p. 160, where the student should experience a shock of recognition if he has read footnote 2. There is no doubt that the Stern–Gerlach experiment, and the Rabi resonance experiment, represent the most elegant, simple, and yet most profound physics experiments of our century.

Problems

1-1. (a) Calculate the vacuum required (in mm Hg) for an atomic beam experiment if the distance from oven to detector is 1 m. Express the result in terms of the cross section σ for collision between a beam atom and a molecule of residual gas. Assume that $\sigma = 10^{-15}$ cm^2 to obtain a quantitative answer.

(b) The atoms in the beam emitted from the oven do not have the same velocity distribution as the atoms in the oven. Show that the beam atoms have a velocity distribution proportional to $v^3 \exp[-3mv^2/2kT]$, where v is the velocity, m is the atomic mass, $k = 1.38 \times 10^{-16}$ ergs°K is Boltzmann's constant, and T is the absolute temperature. Find the most probable velocity and the velocities v_1 and v_2 such that half the atoms in the beam have velocities between v_1 and v_2. Let $T = 500$°K.

(c) Assume the field gradient in the magnet is 10^3 G/cm, and that the magnet is 40 cm long. Assume further that the detector is 50 cm beyond the end of the field gradient region. Find the separation of the two beams of silver atoms for the atoms with the most probable velocity in the beam. Assume $T = 500$°K, and that the width of each beam is as determined in part (b).

1-2. Let the hairpin of Fig. 1-6 be 10 cm long, the separation between the wires 3 mm, and the wires 1 mm in diameter. Find the rf current in the wires necessary to produce a transition from the $m_J = \frac{1}{2}$ to $m_J = -\frac{1}{2}$ state of the ground state of silver for a beam atom of velocity 10^5 cm/sec. What is the width of a resonance line in an apparatus operated under these conditions?

1-3. How far below line of sight does a cesium atom of most probable velocity fall in a 2-m horizontal atomic beam apparatus if the oven temperature is 100°C?

1-4. In our discussion of the Ramsey split field modification of the molecular beam resonance experiment, we assumed the beam molecules to have a single velocity. Discuss qualitatively the consequences to the line shape (Fig. 1-10) if the beam is not monochromatic. Do not forget there are two transit times that may have somewhat different consequences: the time spent in the constant field region between the split rf fields, and the time spent in the rf field region.

References

1. A. Sommerfeld, *Atombau und Spectrallinien*, 4th ed., fr. Vieweg und Sohne, Braunschweig, Germany (1924), p. 145, or 8th ed. (1960), vol. 1, p. 135.
2. N. F. Ramsey, *Molecular Beams*, Oxford University Press, London (1955).
3. H. Kopfermann, *Nuclear Moments*, Academic Press Inc., New York (1958).
4. I. Estermann, O. R. Frisch, and O. Stern, *Nature* **132**, 169 (1933).
5. R. P. Feynman, R. B. Leighton, and M. Sands, *The Feynman Lectures on Physics*, Addison-Wesley, Publishing Co., Reading, Massachusetts (1965), vols. 1, 2, 3.
6. I. Estermann, O. E. Simpson, and O. Stern, *Phys. Rev.* **71**, 238 (1947).
7. O. R. Frisch, *Contemp. Phys.* **1**, 3 (1959).
8. P. Kusch, *Phys. Today* **19**, No. 2, 19 (1966).
9. I. I. Rabi, S. Millman, P. Kusch, and J. R. Zacharias, *Phys. Rev.* **55**, 526 (1939).
10. P. Kusch and H. M. Foley, *Phys. Rev.* **74**, 250 (1948).
11. E. P. Wigner, *Symmetries and Reflections*, Indiana University Press, Bloomington (1967).
12. *Advances in Atomic and Molecular Physics*, D. R. Bates and I. Estermann, Eds., Academic Press Inc., New York, vol. 1 (1965); vol. 2 (1966); vol. 3 (1967); and vol. 4 (1968).

CHAPTER 2

Macroscopic Properties of Nuclear Magnetism

The enormous expansion of the basic ideas of the magnetic resonance technique beyond the molecular beam experiments occurred when it was learned how to do experiments on macroscopic quantities of magnetic moments as found in solids and liquids. There is a considerable difference between flipping an isolated spin from up to down in a molecular beam experiment and doing the analogous thing all at once on 10^{22} spins in ponderable matter. We introduce in this chapter the statistical mechanical steps necessary to describe macroscopic magnetization and its interaction with external electromagnetic fields and with the material in which it is imbedded. The important new idea will be the concept of complex susceptibility, and the practical achievement will be the Bloch equations for the behavior of nuclear magnetism in liquids and some discussion of the apparatus of nuclear magnetic resonance.

2-1. THE EQUILIBRIUM DISTRIBUTION

Chapter 1 has described the basic technique for producing transitions between m_J states of isolated spins. The applications of magnetic resonance in chemistry and solid state physics are based on those methods, but they employ different concepts to produce polarization and to detect the resonance. In this section we shall set forth the basic considerations that govern the relative populations of the different m_J levels when a large number of identical magnetic moments interact with a heat reservoir (usually called a "lattice," even when the moments are in a liquid or a gas). We shall be able to make some very general statements about the way thermal equilibrium is attained, and we shall also derive a few of the macroscopic magnetic properties of the sample, such as its magnetization and magnetic, or Zeeman, energy.

For convenience, we discuss nuclear magnetic moments, which can be nuclei of atoms in a solid, a liquid, or a gas. Much of the discussion will

apply also to electron paramagnets, but they have some properties that present complications requiring rather more specialized discussion, for which we refer the reader to Pake [1]. In the beginning, we further idealize the system of interest by assuming we can neglect the interaction of the moments with each other. We also make a more significant approximation that renders irrelevant the "statistics" of the particles—whether Bose–Einstein or Fermi–Dirac—by requiring the density of the system to be low enough to allow the use of Maxwell–Boltzmann statistics. As a result, we specifically exclude from consideration in this chapter conduction electrons in metals or in liquid ^{3}He at low temperatures. Both systems require the Fermi–Dirac distribution function at low temperatures. Otherwise, for nuclei, the density of ordinary solid matter is easily small enough to allow the Boltzmann distribution to be valid.

We start as simply as possible. Consider N spin $\frac{1}{2}$ nuclei in a magnetic field H_0, applied in the traditional z direction. The population of the $m_I = \pm\frac{1}{2}$ states are N_+ and N_-, with $N_+ + N_- = N$. Now the nuclei, whether in solid, liquid, or gas, have translational degrees of freedom—kinetic and potential energy. Call these degrees of freedom the lattice. Let the lattice be homogeneous; characterize it by a single constant temperature T. Our only other assumption about the lattice is that its heat capacity is large compared with the magnetic energy of interaction of the nuclear moments with the magnetic field. For low temperatures and high fields, this assumption is, in practice, rather restrictive, and the theory developed here must be redone to treat that case. Just how low a temperature and how high a field will be the subject of a problem. Figure 2-1 shows the energy-level diagram and helps define relevant quantities.

The Zeeman energy of each spin is

$$E = -\gamma\hbar H_0 m_I \tag{2-1}$$

If $\gamma > 0$, the $m_I = -\frac{1}{2}$ state is higher in energy. To say anything more, we must assume that the spin system (i.e., the totality of N spins, each

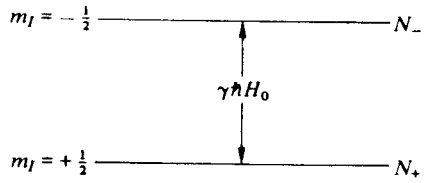

Fig. 2-1 Energy levels of a spin $\frac{1}{2}$ in a magnetic field H_0. Energy levels are ordered for $\gamma > 0$.

interacting with the field H_0) can exchange energy with the lattice. We need not specify the mechanism to make general statements about some of its properties. The lattice must be regarded as a quantum mechanical system with states we label by Greek letters $\alpha, \beta, \ldots$. The states are to be thought of as simple harmonic oscillator levels for atoms bound in a solid. The relative occupation of two levels α and β of energy E_α and E_β is proportional to $\exp[(E_\beta - E_\alpha)/kT]$. If the lattice energy consists of the kinetic energy of translation in a gas, for example, then the energies E_α and E_β refer to the kinetic energy, and the preceding expression is Boltzmann's generalization of the Maxwell velocity distribution. The combined system can be labeled in terms of populations of the various states of the subsystems. The populations are specified by $(N_+, N_-; N_\alpha, N_\beta, \ldots)$. Since the combined systems, Zeeman plus lattice, are assumed isolated from the rest of the universe, an increase in Zeeman energy must be accompanied by an equal decrease in lattice energy.

Figure 2-2 shows two lattice state populations that differ by the Zeeman

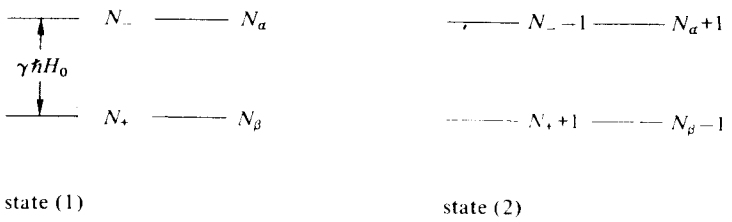

Fig. 2-2 Energy levels for system of spin $\frac{1}{2}$ and a pair of lattice levels with same energy difference. States (1) and (2) of the combined system have the same energy.

energy $\hbar\gamma H_0$, and it indicates schematically two populations of the combined system that have the same energy. Part (1) has the higher Zeeman energy of the two; (2) has the higher lattice energy. We postulate that there is a rate process, determined by a transition rate W, which connects pairs of states the Zeeman populations of which differ by one spin being turned over. We write the following equations for the time rate of change of the spin populations:

$$\frac{dN_+}{dt} = -N_+ W(+ \rightarrow -) + N_- W(- \rightarrow +) \tag{2-2}$$

and

$$\frac{dN_-}{dt} = -\frac{dN_+}{dt} \tag{2-3}$$

since $N_+ + N_- = N$. Remember that the transition rate $W(+ \rightarrow -)$, for example, involves implicitly a transition from (2) to (1) of Fig. 2-2, *including* the redistribution of lattice-level populations.

The thermal equilibrium condition is $dN_+/dt = 0$, from which we conclude that

$$\frac{N_+^0}{N_-^0} = \frac{W(- \rightarrow +)}{W(+ \rightarrow -)} \tag{2-4}$$

where the superscripts indicate thermal equilibrium. On the other hand, the total number of transitions per second of the entire system from (1) to (2) is given by

$$\text{trans/sec from (1) to (2)} = N_- N_\beta w \tag{2-5}$$

where w is a quantum mechanical transition probability involving *only* the squares of matrix elements, densities of states, and constants. The import of the consitution of w is that it is microscopically reversible; w appears in the equivalent expression for the total number of transitions per second from (2) to (1):

$$\text{trans/sec from (2) to (1)} = N_+ N_\alpha w \tag{2-6}$$

In thermal equilibrium, the quantities calculated in (2-5) and (2-6) are equal, from which we conclude

$$\frac{N_+^0}{N_-^0} = \frac{N_\beta}{N_\alpha} \tag{2-7}$$

That is, the Zeeman state population ratio is the same as the population ratio of any pair of lattice states separated by the Zeeman energy. This latter ratio is, except for the case of very low temperatures alluded to earlier,

$$\frac{N_\beta}{N_\alpha} = \frac{\exp(-E_\beta/kT)}{\exp(-E_\alpha/kT)} = \exp\frac{-(E_\beta - E_\alpha)}{kT} \tag{2-8}$$

From Eqs. (2-1), (2-7), and (2-8), and from Fig. (2-2), we have

$$\frac{N_+^0}{N_-^0} = \exp\frac{-(E_+ - E_-)}{kT} = \exp\frac{+\gamma\hbar H_0}{kT} \tag{2-9}$$

That is, the lower energy level of the spin system, $m_I = +\frac{1}{2}$, is more highly occupied in thermal equilibrium. Moreover, from Eq. (2-3) we get

$$\frac{W(- \rightarrow +)}{W(+ \rightarrow -)} = \exp \frac{\gamma \hbar H_0}{kT} \tag{2-10}$$

Downward transitions are more probable; indeed, you can look at Eq. (2-10) as providing the mechanism whereby the equilibrium population ratio (2-9) is produced and maintained.

We may now return to (2-3) and talk about the approach to equilibrium from a nonequilibrium initial condition. Define the population difference

$$n = N_+ - N_- \tag{2-11}$$

and rewrite N_+ and N_- in terms of n and N:

$$N_+ = \tfrac{1}{2}(N + n) \tag{2-12a}$$

$$N_- = \tfrac{1}{2}(N - n) \tag{2-12b}$$

In terms of N and n, Eq. (2-3) becomes

$$\frac{dn}{dt} = N[W(- \rightarrow +) - W(+ \rightarrow -)] - n[W(+ \rightarrow -) + W(- \rightarrow +)] \tag{2-13}$$

or, by factoring out $[W(+ \rightarrow -) + W(- \rightarrow +)]$,

$$\frac{dn}{dt} = \frac{n_0 - n}{T_1} \tag{2-14}$$

where

$$n_0 = N \frac{W(- \rightarrow +) - W(+ \rightarrow -)}{W(+ \rightarrow -) + W(- \rightarrow +)} \tag{2-15}$$

and

$$\frac{1}{T_1} = W(+ \rightarrow -) + W(- \rightarrow +) \tag{2-16}$$

where n_0 is the equilibrium population difference, as substitution of (2-10) and (2-11) into (2-15) will verify:

$$n_0 = N \frac{W(+ \rightarrow -)[\exp(\gamma \hbar H_0/kT) - 1]}{W(+ \rightarrow -)[\exp(\gamma \hbar H_0/kT) + 1]} = N \tanh\left(\frac{\gamma \hbar H_0}{2kT}\right) \tag{2-17}$$

The time T_1, defined by (2-16), is the spin lattice relaxation time; it is the time constant of the approach of the spin system to thermal equilibrium with the lattice. If (2-14) is solved with $n(0) = 0$ as the initial condition, as would be the case if the field were switched on suddenly at $t = 0$ after having always been zero before, we find that

$$n = n_0[1 - \exp(-t/T_1)]$$

It is appropriate at this point to put in perspective what we have been doing, and perhaps even allow a glimpse of a skeleton in a closet. Equations (2-3), (2-5), and (2-6) are examples of the *principle of detailed balance*, which was first used by Einstein in his 1916 rederivation of the Planck radiation formula. Given Eq. (2-2), which is also known as a *master equation*, the irreversibility of the approach to equilibrium is already determined, even though (2-2) makes explicit use of the microscopically reversible quantum mechanical transition probability w, introduced in Eq. (2-5). The justification, or, if you wish, derivation of the master equation is the central problem of nonequilibrium statistical mechanics. Magnetic resonance experiments on nuclear spin systems in solids and liquids have in recent years provided interesting and tractable model systems for which specific derivations of equations such as Eq. (2-3) could be tested, and the limitations understood.

Although it is rather far afield from our main purpose, something more than the preceding mysterious remarks can be made with regard to the origin of the irreversibility. In terms of the coefficients a and b introduced in Chapter 1 for the spin wave functions $|\chi\rangle = a|\frac{1}{2}\rangle + b|-\frac{1}{2}\rangle$, it is clear that (2-2) is an equation in $|a|^2$ and $|b|^2$, since the probability of occupation of a given stage for a single spin is essentially $(1/N)$ times the occupation of that state in the ensemble of N identical spins. The information that is missing is the relative phase of the $|\frac{1}{2}\rangle$ and $|-\frac{1}{2}\rangle$ states, which, if we remember Chapter 1, is related to the transverse component of the magnetic moment. In equilibrium there is no transverse macroscopic magnetic moment, not even a coherent alternating one. From that, we reason backward to the conclusion that the relative phase of the $m_I = +\frac{1}{2}$ states from spin to spin must be a random quantity, so that the total transverse moment vanishes. The reasoning is purposely circular, but it points to the crux of the problem and reintroduces the idea that a macroscopic transverse magnetization, such as produced in a magnetic resonance experiment, has to do with a coherent admixture, from spin to spin, of the magnetic states m_I.

2-2. ENERGY, MAGNETIZATION, AND SUSCEPTIBILITY

The magnetic energy, or Zeeman energy, of the spin system is given for a general spin I by

$$E = \sum_{m_I=-I}^{I} E(m_I)N(m_I) \tag{2-18}$$

It is convenient to define the zero of energy $E(m_I)$ for each spin to be at $m_I = 0$ for I even, and midway between the $m_I = \pm\frac{1}{2}$ energy levels for I an odd half-integer. Then Eq. (2-1) is the appropriate expression for $E(m_I)$ in Eq. (2-18). For $N(m_I)$, we shall simplify matters a little by using an expression that will be valid in the high temperature limit only: $\gamma\hbar H_0 \ll kT$.

$$N(m_I) = \frac{N \exp(-\hbar\gamma m_I H_0/kT)}{\sum_{-I}^{I} \exp(-\hbar\gamma m_I H_0/kT)} \cong \frac{N}{2I+1} \exp\frac{-\hbar\gamma m_I H_0}{kT} \tag{2-19}$$

The first equation in expression (2-19) is, of course, exact. The denominator is that fundamental expression of statistical mechanics, the "sum over states," or partition function. The replacement of the denominator by $2I + 1$ in the second equation in (2-19), although retaining the full exponential expression in the numerator, is conventional but inconsistent. If $\gamma\hbar H_0 m_I/kT \ll 1$, the exponential in the denominator may be expanded:

$$\sum_{-I}^{I} \exp\frac{-\gamma\hbar H_0 m_I}{kT} = (2I+1) - \frac{\gamma\hbar H_0}{kT}\sum_{-I}^{I} m_I + \frac{1}{2}\left(\frac{\gamma\hbar H_0}{kT}\right)^2 \sum_{-I}^{I} m_I^2 + \cdots$$

The second term in the sum is zero since $\sum m_I = 0$, but the next term is not. Thus, the denominator's lowest term in the expansion parameter is quadratic, but the numerator's lowest term is linear. To be consistent, we must take two terms of the numerator and one of the denominator. The exponent in the numerator has been retained at this stage because one so often is concerned with population ratios, in which case it is somehow easier always to write

$$\frac{\exp(E_\alpha/kT)}{\exp(E_\beta/kT)} = \exp\frac{(E_\alpha - E_\beta)}{kT} \cong 1 + \frac{E_\alpha - E_\beta}{kT}$$

than

$$\frac{1 + (E_\alpha/kT)}{1 + (E_\beta/kT)} \simeq \left(1 + \frac{E_\alpha}{kT}\right)\left(1 - \frac{E_\beta}{kT}\right) \simeq 1 + \frac{E_\alpha - E_\beta}{kT}$$

Equation (2-19) satisfies Eq. (2-9), agrees with (2-17) in the high temperature limit, and satisfies conservation of spins, $\sum_{-I}^{I} N(m_I) = N$, in that limit also. Expansion of (2-18) with (2-19) in the high temperature limit yields

$$E \simeq \frac{N}{2I+1}\sum_{-I}^{I} \gamma\hbar H_0 m_I\left(1 - \frac{\gamma\hbar H_0}{kT} m_I\right)$$
$$= -\frac{N}{2I+1}\left(\frac{\hbar H_0}{kT}\right)^2 \sum_{-I}^{I} m_I^2$$

It is easily verified that $\sum_{-I}^{I} m_I^2 = [I(I+1)(2I+1)]/3$, so that

$$E = \frac{N\gamma^2\hbar^2 I(I+1)H_0^2}{3kT} \tag{2-20}$$

As an aside, it is interesting to compare the formula (2-20) with the classical formula in the same limit:

$$E = -\langle \boldsymbol{\mu} \cdot \mathbf{H}_0 \rangle N = \mu H_0 N\langle \cos\theta \rangle \tag{2-21}$$

where $\langle\ \rangle$ indicates the thermal average of the quantity inside it, calculated according to Boltzmann statistics. To find $\langle\cos\theta\rangle$, one must weight $\cos\theta$ by the probability that the moment μ is oriented at angle θ to H_0:

$$\langle\cos\theta\rangle = \frac{\int_\Omega \cos\theta \exp(\mu H_0 \cos\theta/kT)\, d\Omega}{4\pi}$$

where the integration is over the solid angle the complete range of which is the denominator 4π. Expand the exponential. The first term vanishes and the second yields:

$$\frac{\mu H_0}{kT}\frac{1}{2}\int_0^\pi d\theta \cos^2\theta \sin\theta = \frac{1}{3}\frac{\mu H_0}{kT}$$

Substituting back into (2-21), we obtain

$$E = \frac{-N\mu^2 H_0^2}{3kT}$$

The quantum mechanical equivalent of μ^2 is $\gamma^2\hbar^2 I(I+1)$,[1] and the factor

[1] Occasionally one sees the quantity $[g^2 I(I+1)]^{1/2}$ defined to be the magnetic moment, rather than gI. The former is most frequently found in the older literature on magnetism.

of 3 in the denominator of (2-20) is the quantum average of m_I^2, just as it is the average of $\cos^2\theta$ in the classical calculation. (This equivalence was known as the "principle of spectroscopic stability" in the early days of quantum mechanics.)

The magnetic moment per unit volume may be defined by the expression $E/V = -\mathbf{M}_0 \cdot \mathbf{H}_0$. From (2-20), we see that

$$\mathbf{M}_0 = \frac{N}{V}\frac{\gamma^2\hbar^2 I(I+1)}{3kT}\mathbf{H}_0 \tag{2-22}$$

The same expression is obtained from $M_0 = n_0\mu_z/V$, where n_0 is given by the high temperature expansion of (2-17). The static magnetic susceptibility χ is defined by $\mathbf{M}_0 = \chi_0\mathbf{H}_0$, so we obtain the well-known formula

$$\chi_0 = \left(\frac{N}{V}\right)\frac{\gamma^2\hbar^2 I(I+1)}{3kT} \tag{2-23}$$

A word about units is in order. In the Gaussian system, which is still largely used in research physics even though it is no longer the system of choice in elementary courses, the dimensions of M, B, and H are the same. Hence, χ_0, from the defining expression, is dimensionless. As defined here, it is often referred to as the *volume susceptibility*, however, to distinguish it from *mass* or *molar* susceptibilities. These quantities arise from a definition of M_0 in which the number of moments contributing is not the number in cubic centimeters, as in (2-22), but the number in a gram or the number in a mole. With such a definition, since M_0 and H_0 must still have the same dimensions, the quantity χ_0 is not necessarily dimensionless. The mass and molar susceptibilities are related to the volume (i.e., dimensionless) susceptibility by

$$(\chi)_{\text{mass}} = \frac{(\chi)_{\text{vol}}}{\rho} \tag{2-24a}$$

$$(\chi)_{\text{molar}} = (\chi)_{\text{vol}}\, v \tag{2-24b}$$

where ρ in (2-24a) is the density, and v in (2-24b) is the molar volume, $v = N_A M/\rho$, where N_A is Avogadro's number, and M is the atomic mass.

2-3. RESPONSE TO AN ALTERNATING FIELD; COMPLEX SUSCEPTIBILITIES

In the Rabi magnetic resonance experiment, isolated spins interacted only with the static and alternating fields. Earlier in this chapter we introduced the concept of spin-lattice interaction. We now need to

combine them all and discuss, as we did before, the components of the magnetic moment in the presence of these interactions. Now, however, the magnetic moment to consider is the macroscopic magnetic moment of the entire sample. We shall begin by discussing the z component, followed by the transverse components M_x and M_y.

There is a subtle difference between the effect of the rf field on the isolated atom in Eq. (1-22) and its effect in the presence of spin-lattice interaction. The origin of the distinction lies in the fact that with spin-lattice interaction the states m_I are not quite eigenstates of the total Hamiltonian. When one speaks of the states in the approximate language of m_I, one must then absorb the approximate nature of the description into a lack of sharpness of the energy level, and one speaks of the level as having a breadth given, in fact, by the uncertainty principle argument $\Delta E > \hbar/T_1$. In discussing M in the presence of the rf field, we are particularly interested in small deviations of M from M_0. The rf field is regarded as a perturbation that, in the language of Chapter 1, is to produce only a small amplitude b in a state which initially had $|a|^2 = 1$. Thus, in Eq. (1-22), $P(\frac{1}{2}) \ll 1$ in the perturbation theory limit, if $|a|^2 \simeq 1$ is to continue to be true. $P(-\frac{1}{2})$ is small for small times t after the perturbation is turned on, and one sees immediately that $P(-\frac{1}{2}) \simeq t^2$ for intervals of t such that $P(-\frac{1}{2}) \ll 1$. Fortunately for the preservation of a linear theory, the quadratic dependence on t is not correct for the problem with which we are now concerned, and the correct time dependence for the probability of the $m_I = -\frac{1}{2}$ state being occupied is a linear rather than a quadratic one. The apparent paradox is resolved by noting that $P(-\frac{1}{2})$ was computed for exact eigenstates $m_I = \pm\frac{1}{2}$, whereas these are not exact eigenstates in the presence of spin-lattice relaxation. The final result must involve an integration over all the states making up the "level" of nonzero width. The details are carried out in Abragam's treatise *Nuclear Magnetism* [2] (see Chapter 2).

The probability of a transition from the state m_I to the state $m_I - 1$ is proportional to time. Unlike the case of spin-lattice relaxation, however, the transition rate for a spin in state $m_I - 1$ to m_I is the same as the transition rate for a spin in state m_I to $m_I - 1$. The processes are to be contrasted: the spin-lattice relaxation process drives the population difference n toward the thermal equilibrium value n_0; the rf field drives n toward zero. The latter statement is easily verified:

$$\left(\frac{dN_+}{dt}\right)_{\text{rf}} = -N_+ W_{\text{rf}} + N_- W_{\text{rf}} = -nW_{\text{rf}}$$

and

$$\left(\frac{dN_-}{dt}\right)_{\text{rf}} = -\left(\frac{dN_+}{dt}\right)_{\text{rf}}$$

Hence,

$$\left(\frac{dn}{dt}\right)_{rf} = -2W_{rf}\,n \tag{2-25}$$

Equilibrium occurs when $n = 0$, Q.E.D. The transition probability per unit time W_{rf} is properly computed by the standard time dependent perturbation formula (the so-called "golden rule") of quantum mechanics. The perturbation is the interaction of the magnetic moment and the rf field, $-\boldsymbol{\mu} \cdot \mathbf{H}_1$; we need remark here only that W_{rf} is proportional to ${H_1}^2$.

The total rate of change of n is the sum of (2-14) and (2-25)

$$\frac{dn}{dt} = -2W_{rf}\,n + \frac{n_0 - n}{T_1} \tag{2-26}$$

In the steady state $dn/dt = 0$, and (2-26) shows that

$$n = \frac{n_0}{1 + 2W_{rf}\,T_1} \tag{2-27}$$

Equations (2-26) and (2-27) may be rewritten in terms of $M_z = n\gamma\hbar/2$ simply by substituting M_z for n and M_0 for n_0. Equation (2-27) shows that the rf field does not appreciably disturb M_z from M_0 as long as $2W_{rf}T_1 \ll 1$. When this inequality is not satisfied, $n < n_0$, and the resonance is said to be *saturated*. Additionally, the rate of energy absorption from the rf field may be calculated from (2-26),

$$\frac{dE}{dt} = \hbar\omega n W_{rf} = \frac{n_0\,\hbar\omega W_{rf}}{1 + 2W_{rf}\,T_1} \tag{2-28}$$

Note that dE/dt becomes independent of W_{rf} as W_{rf} exceeds $\frac{1}{2}T_1$.[2]

The discussion of the transverse components of M in the steady state situation must be phrased in rather general terms. It is again convenient to work in the frame rotating with the rf field, angular frequency ω. Let H_1 be along the x axis in the rotating frame. Define susceptibilities χ' and χ'' by the relations

$$M_x = 2\chi' H_1 \tag{2-29a}$$

$$M_y = 2\chi'' H_1 \tag{2-29b}$$

Equations (2-29) are, first of all, linear. That is, the transverse magnetization is proportional to the first power of the perturbing rf field H_1. Note that χ' has been defined to be the proportionality factor between H_1 and

[2] The failure of the first attempts to observe nuclear magnetic resonance in solids, by C. J. Gorter in the late 1930's, can be traced to the use of a sample with a T_1 that probably was several hours, so that $2W_{rf}T_1$ was undoubtedly very large and the power absorbed from the rf field by the sample was very small.

the component of M parallel to, or in phase with, H_1 in the rotating frame. The out-of-phase or orthogonal component is determined by χ''.

Necessary additional insight is obtained by transforming back to the laboratory frame, X, Y, $Z = z$, where we assume that the rotating H_1 is produced by a linearly polarized rf field in the X direction:

$$H_x(t) = 2H_1 \cos\omega t$$

In the laboratory frame, then, the X component of the magnetization is, from Eq. (2-29),

$$M_X(t) = (\chi' \cos\omega t + \chi'' \sin\omega t)2H_1 \tag{2-30}$$

Equation (2-30) may be expressed more compactly, and more conventionally, as the real part of a complex quantity. We define the complex quantities $\mathscr{H}_X = 2H_1 e^{i\omega t}$ and $\mathscr{M}_X = 2\chi H_1 e^{i\omega t}$. Their real parts are the physical field and magnetization, respectively. Comparison with Eq. (2-30) shows that $M_X = \mathrm{Re}\,\mathscr{M}_X$ only if χ is the complex quantity

$$\chi = \chi' - i\chi'' \tag{2-31}$$

The linear relation between the complex driving term $\mathscr{H}_X(t)$ and the complex response function $\mathscr{M}_X(t)$ has many familiar parallels in physics. Probably the first one encountered by most students is the generalized Ohm's law from ac circuit theory, $\mathscr{V} = \mathscr{I}\,\mathscr{Z}$, where $\mathscr{Z}$ is the complex impedance. The same care must be used in calculating quantities with complex $\mathscr{M}$ and $\mathscr{H}$, as with complex current, impedance, and voltage. Thus the instantaneous power absorbed from a generator is (Re $\mathscr{M}$) (Re $\mathscr{H}$), not Re($\mathscr{M}\mathscr{H}$).

The average power absorbed by a unit volume of material is

$$P = \frac{1}{T}\int_0^T \mathrm{Re}\,\mathscr{H} \cdot \mathrm{Re}\left(\frac{d\mathscr{M}}{dt}\right) dt \tag{2-32}$$

where $T = 2\pi/\omega$ is an rf period. The only term in the scalar product in the integrand is the X component, so

$$P = \frac{1}{T}\int_0^T (2H_1)^2 \cos\omega t(-\omega\chi' \sin\omega t + \omega\chi'' \cos\omega t)\,dt$$

$$= 4{H_1}^2\omega\chi''\left(\frac{1}{T}\int_0^T \cos^2\omega t\,dt\right) = 2{H_1}^2\omega\chi'' \tag{2-33}[3]$$

[3] Comparison with Eq. (2-28) would allow immediate determination of χ'' if W_{rf} were known. We shall not pursue that course, since we shall eventually get W_{rf}, for the particular situation (2-28) represents (lifetime broadened levels) without using quantum mechanical perturbation theory. See the discussion at the end of Section 2-5.

The analogy between the impedance and χ cannot be made blindly. The real part of $\mathscr{Z}$ determines the loss, and the imaginary part determines the nature of the periodic but lossless exchange of energy between the circuit and the generator. The terms "real" and "imaginary" must be interchanged in the preceding discussion because the voltages that interact with currents in the magnetic system are *induced*; they are determined by $d\mathscr{M}/dt = i\omega\mathscr{M}$. The phenomenon of induction accounts for the factor of ω in (2-33) and the appearance of χ'' instead of χ' in the expression for the absorbed power.

Without further assumptions about the details of the system, except for the all-important one that the "cause must precede the effect," one can establish that χ' and χ'' are not independent of each other but are related by integral relations known as the Kramers–Kronig relations, which were independently derived with reference to optical absorption by Kramers and Kronig in 1926. A thorough discussion and derivation of these relations may be found in the text by Slichter [3], in which there is a precise mathematical formulation of the somewhat enigmatic statement made previously about cause and effect. Relations such as those of Kramers and Kronig exist between the real and imaginary parts of the complex linear response functions of physical systems, whether they be magnetic or electric susceptibilities, impedances of passive electrical circuits, or reactions in elementary particle physics.

2-4. THE BLOCH EQUATIONS

Nuclear magnetic resonance in condensed material (namely, hydrogenous materials such as water or paraffin wax) was first observed in 1946 independently by Professor Felix Bloch and coworkers at Stanford, and Professor E. M. Purcell and coworkers at Harvard.[4] In conjunction with the experiments at Stanford, Bloch proposed phenomenological equations of motion for the macroscopic magnetization vector **M**, which serve very well to describe magnetic resonance experiments in liquids, gases, or "liquidlike" solids. It will be one of the tasks of this book to enable the student to comprehend in physical terms the limitations of the Bloch equations, but first we must set them down and explore their solutions.

The object is to express the interaction of the magnetization with the external fields (static and alternating), with the lattice, and to write a term that expresses the interaction of the magnetic moments with each other and with other *internal* magnetic fields in the sample. We have already accomplished the first two tasks, and we have a major portion of the Bloch

[4] Bloch and Purcell shared the 1952 Nobel prize for their work, the third Nobel prize awarded for work described in this book. Stern won the prize for his molecular beam work in 1943, and Rabi for the magnetic resonance method in 1944.

equations if we assemble Eqs. (1-11) and (2-26) in slightly altered and compatible form. The effect of the interaction of the moments undergoing resonance with each other and other magnetic moments in the sample, via the dipole-dipole interaction or through more esoteric quantum mechanical effects called exchange interactions, is contained within the Bloch equations by a single parameter that affects only the transverse magnetization, the components of which are M_x and M_y. (We shall use lowercase subscripts for the laboratory coordinate system in this section, and identify equations written in the rotating system explicitly.)

Bloch assumed that the internal interactions of spins with each other could be expressed by the equation

$$\frac{\partial M_{x,y}}{\partial t} = -\frac{M_{x,y}}{T_2} \tag{2-34}$$

Equation (2-34) defines the parameter T_2, known variously as the transverse or spin-spin relaxation time. (The partial derivative has been written only to call particular attention to the existence of the other terms that cause $M_{x,y}$ to change.) Equation (2-34) is the equation for a magnetization that decays exponentially to zero. Suppose that in the rotating frame at $\omega_0 = \gamma H_0$ the transverse component M_x is created at $t = 0$. In the context of Chapter 1 it persisted indefinitely. What can cause it to decay? One obvious cause would be an inhomogeneous magnetic field across the sample so distributed that the Larmor frequencies of the spins in the various parts of the sample differ sufficiently so that in time T_2 they would get out of phase with each other enough to diminish the initial M_x to $1/e$ of its value. Although it would take special field inhomogeneity to make the magnetization decay exactly exponentially, the point is worth illustrating with a figure. Figure 2-3 shows $M_x(0)$, in the rotating frame. Imagine

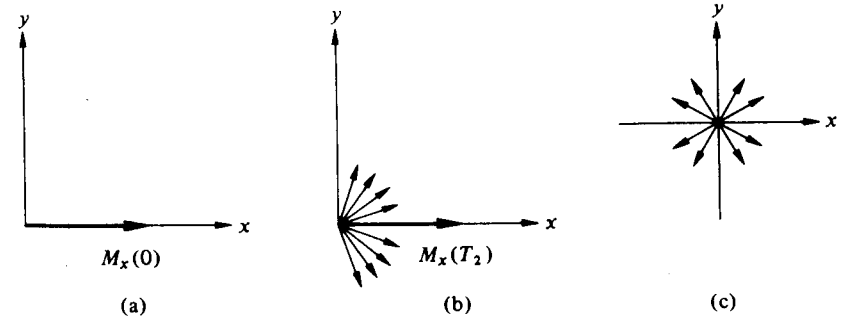

Fig. 2-3 Rotating frame view of decay of M_x. (a) Initial condition. (b) Partial decay ($t \sim T_2$). (c) Total decay ($t \gg T_2$).

M_x made up of small magnetization vectors that precess at a variety of frequencies differing by small amounts either way from the average frequency ω_0. Then in a frame rotating at ω_0, they precess one way or the other until by $t = T_2$, their vector sum is still in the x direction but has diminished to $M_x(0)/e$.

One internal physical process that diminishes the transverse magnetization is the spin-lattice relaxation time T_1. Any other process, such as field inhomogeneity, only adds to the rate at which $M_{x,y}$ diminishes, so that $T_2 < T_1$. The most interesting T_2 process is the interaction of each spin with internal fields. By analogy with the external field inhomogeneity mechanism, we should guess that the internal fields that act to dephase $M_{x,y}$ are those parts of the total internal fields which are in the z direction and which are static and quasistatic. That the internal fields should manifest themselves just as single parameter T_2 in an equation of the form of Eq. (2-34) is, in fact, a result of rather special circumstances which we shall explore later.

Combining Eq. (2-34) with the torque and relaxation equations, we get the Bloch equations:

$$\frac{dM_z}{dt} = \frac{M_0 - M_z}{T_1} + \gamma(\mathbf{M} \times \mathbf{H})_z \tag{2-35a}$$

$$\frac{dM_{x,y}}{dt} = -\frac{M_{x,y}}{T_2} + \gamma(\mathbf{M} \times \mathbf{H})_{x,y} \tag{2-35b}$$

where

$$\mathbf{H} = \hat{\mathbf{k}}H_0 + \hat{\mathbf{i}}H_1(t)$$

2-5. SOLUTIONS OF THE BLOCH EQUATIONS

Solutions of Eqs. (2-35) are not difficult to obtain for a few special experimental conditions that are also of particular interest in practice. We have actually already discussed, in two separate parts, one particularly interesting solution that we can do without mathematics; thus we begin with that example.

Free induction decay

In making the plausibility argument for the form of the T_2 term, we began arbitrarily with the magnetization in the x direction in the rotating frame. The subsequent exponential decay with time constant T_2, determined by Eq. (2-34), appears in the laboratory frame as

$$M_x(t) = M_{x0} \cos \omega_0 t \exp \frac{-t}{T_2} \tag{2-36}$$

We have two problems: how to produce $M_x(0)$ and how to detect $M_x(t)$. Producing $M_x(0)$ may be accomplished by a "90° pulse," a transverse rf pulse of magnitude H_1 in the rotating frame at $\omega_0 = \gamma H_0$, which acts for a time τ such that $\gamma H_1 \tau = \pi/2$. From Chapter 1 we see that if H_1 is stationary in the y direction in the rotating frame, $M_z = M_0$ precesses about H_1 at $\gamma H_1 = \omega_1$ until, at $\tau = \pi/2\gamma H_1$, it is pointing in the $-x$ direction. The experimental arrangement to do this is shown in Fig. 2-4. We have neglected one thing of great importance. The pulsed rf field that produces the 90° rotation of M_0 in the rotating frame must act in the presence of T_1 and T_2 processes, rather than in their absence, as in Chapter 1. Consequently, the 90° nutation of M_0 is only an approximate description of what happens, and we must find how good an approximation it is. If the major torque on the magnetization is to be from H_1 during $0 < t < \tau$, then the relaxation toward H_0 (in time T_1) and the dephasing of the transverse magnetization (in time T_2) must not be important compared to the precession about H_1 during τ: $\tau \ll T_2 < T_1$. The requirement on H_1 is thus $(\pi/2\gamma H_1) \ll T_2$, or

$$\gamma H_1 \gg \frac{\pi}{2T_2} \tag{2-37}$$

It is the same result we get if we assume, plausibly, that H_1 must be much larger than the internal fields or external field inhomogeneities described by T_2.

A word is in order about the magnitudes involved for a nuclear resonance experiment. The largest internal fields in ordinary substances (think of NaCl, for example) are caused by the nuclear magnetic dipole-dipole interaction. The magnetic field produced by one dipole a distance r from another is on the order of μ/r^3. Typically, since $\mu \cong \gamma\hbar = 10^{-23}$ ergs/G, and $r \sim 2 \times 10^{-8}$ cm, $\Delta H = \mu/r^3 \cong 10^{-23}/8 \times 10^{-24} \cong 1$ G. Although the Bloch equations are not, in fact, generally valid for solids, they do provide a framework for rapid estimates of upper or lower limits. To satisfy our inequalities, $H_1 \gtrsim 10$ G is required, and $\tau < \pi/(2 \times 10^4 \times 10) \cong 10$ μsec. The T_2 for this case is about $T_2 \sim 1/\gamma\,\Delta H = 100$ μsec. These calculations provide upper limits on fields and lower limits on times for this particular substance, because, as we shall see in the next chapter, the effect of the nuclear motion that occurs in a liquid or gas is to decrease the effective dipole-dipole interaction for T_2 processes, often by several orders of magnitude.

How large is the induced signal? The precessing magnetization in the xy plane in the laboratory frame is of initial magnitude $M_0 = \chi_0 H_0$, where χ_0 is the static susceptibility, Eq. (2-23). Referring to Fig. 2-4, let the coil that produced the 90° pulse of H_1 serve also to pick up the induced

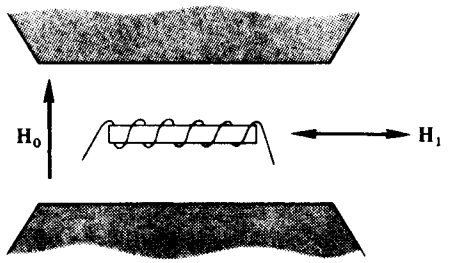

(a) field geometry

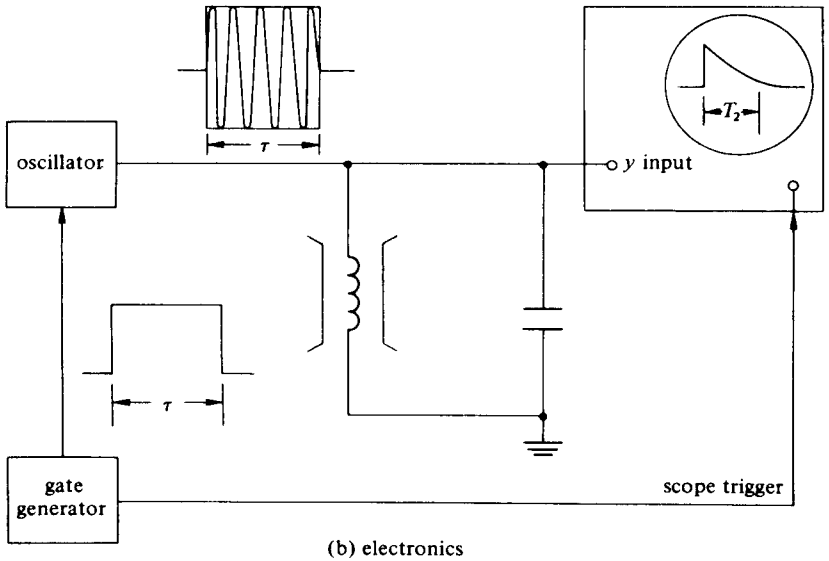

(b) electronics

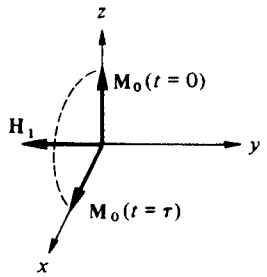

(c)

Fig. 2-4 Schematized apparatus for observing nuclear free induction decay. (a) Field geometry. (b) Electronics. (c) Rotating frame field and magnetization vectors.

signal caused by the rotating magnetization immediately after the 90° pulse. If the coil is of unit volume, cross-section area A, and has n turns, then the induced voltage will be

$$V_0 = -\frac{n}{c}\eta\frac{d\phi}{dt} = -\frac{1}{c}4\pi An\eta\frac{dM}{dt} = -\frac{1}{c}4\pi n\eta A\omega M_0 \qquad (2\text{-}38)$$

where ϕ is the flux linking the coil: $\phi = BA$, and $B = 4\pi M$, and η is a factor between zero and one, the "filling factor," which takes into account incomplete flux linkage between sample and coil. A problem at the end of the chapter will show that the magnitude of V can be as large as several millivolts for nuclear systems if the coil is part of a resonant circuit of reasonable Q.[5] Several millivolts is, of course, a very easily detectable signal at radio frequencies.

Equation (2-38) gives the signal V_0 immediately after the 90° pulse, where the full equilibrium magnetization M_0 is turned over into the transverse plane. The transverse magnetization, as we have seen, decays exponentially with a time constant T_2. Since $T_2 \gg 2\pi/\omega_0$, the signal is contained within a slowly varying envelope. The envelope decays according to the expression $V_0 \exp(-t/T_2)$, which is known as the "free induction decay."

Steady state solution

The next type of solution of the Bloch equations to investigate is the steady state solution in the presence of continuous H_1. We shall express the solutions of (2-35) in terms of the susceptibilities $\chi'(\omega)$ and $\chi''(\omega)$. To begin, we rewrite Eqs. (2-35) in component form in the rotating frame of the rf field, which, in the laboratory frame, is

$$\mathbf{H}_1(t) = \mathbf{i}2H_1\cos\omega t$$

The transformation is defined by $\boldsymbol{\omega} = -\omega\mathbf{k}$. We ignore the counter-rotating component, as in Chapter 1.

$$\frac{dM_z}{dt} = -\gamma M_y H_1 + \frac{M_0 - M_z}{T_1} \qquad (2\text{-}39a)$$

$$\frac{dM_x}{dt} = -\gamma M_y\left(H_0 - \frac{\omega}{\gamma}\right) - \frac{M_x}{T_2} \qquad (2\text{-}39b)$$

$$\frac{dM_y}{dt} = -\gamma\left[M_z H_1 - M_x\left(H_0 - \frac{\omega}{\gamma}\right)\right] - \frac{M_y}{T_2} \qquad (2\text{-}39c)$$

[5] The results of Eq. (2-38) will be in the Gaussian units, where V is expressed in statvolts. The result must be multiplied by 300 to express the results in volts.

In the steady state, the left-hand sides of Eqs. (2-39) vanish. From Eq. (2-39a) we see that $(M_0 - M_z)$ is proportional to $M_y H_1$. We expect, from the definitions of the susceptibilities χ' and χ'', that M_y will be proportional to H_1, so $(M_0 - M_z)$ is of the order ${H_1}^2$. As long as we restrict ourselves to terms linear in H_1, we can replace M_z by M_0 in Eqs. (2-39b) and (2-39c).

The algebra is simplified by introducing $\mathcal{M}_+ = M_x + iM_y$. Add (2-39b) to $\sqrt{-1} = i$ times (2-39c):

$$\frac{d\mathcal{M}_+}{dt} = -\mathcal{M}_+ \left[\frac{1}{T_2} + i\gamma\left(H_0 - \frac{\omega}{\gamma}\right)\right] + i\gamma M_0 H_1 \qquad (2\text{-}40)$$

The steady state solution to Eq. (2-40) is

$$\mathcal{M}_+ = \frac{i\gamma M_0 H_1}{1/T_2 + i\gamma(H_0 - \omega/\gamma)} \qquad (2\text{-}41)$$

We define $\omega_0 = \gamma H_0$, substitute $M_0 = \chi_0 H_0$, and then separate into real and imaginary parts to get

$$M_x = \chi_0 \omega_0 T_2 \frac{(\omega_0 - \omega)T_2}{1 + (\omega - \omega_0)^2 {T_2}^2} H_1 \qquad (2\text{-}42a)$$

$$M_y = \chi_0 \omega_0 T_2 \frac{1}{1 + (\omega - \omega_0)^2 {T_2}^2} H_1 \qquad (2\text{-}42b)$$

From the definitions of χ' and χ'', Eq. (2-30), we identify the components of the complex susceptibility:

$$\chi' = \frac{\chi_0 \omega_0 T_2}{2} \quad \frac{(\omega_0 - \omega)T_2}{1 + (\omega - \omega_0)^2 {T_2}^2} \qquad (2\text{-}43a)$$

$$\chi'' = \frac{\chi_0 \omega_0 T_2}{2} \quad \frac{1}{1 + (\omega - \omega_0)^2 {T_2}^2} \qquad (2\text{-}43b)$$

In Fig. 2-5, χ' and χ'' are plotted versus $(\omega_0 - \omega)T_2$.

The components of the complex susceptibilities have some interesting features. The full width at half-maximum of the absorption χ'' is $2/T_2$, and the peaks of the dispersion χ' are at $\omega = \omega_0 \pm 1/T_2$. Equations (2-43) are called Lorentz curves, after the line shape of the optical absorption and emission predicted by Lorentz using a damped simple harmonic

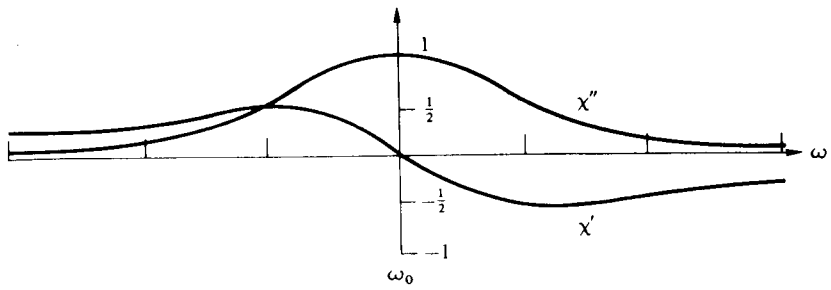

Fig. 2-5 The rf susceptibilities χ' and χ'' as a function of radio frequency ω. The vertical scale is in units of $\chi_0 \omega_0 T_2/2$; the horizontal axis is in units of $1/T_2$.

oscillator model of the atom. The power of the resonance technique is illustrated by the observation that the maximum value of χ'', $\chi_0 \omega_0 T_2/2$, may be written $\chi_0 H_0/\Delta H$, where $\Delta H = 2/\gamma T_2$ is the full width of χ'' in field units. In liquids, T_2 can be on the order of seconds, and hence the factor $\omega_0 T_2/2$ or $H_0/\Delta H$ can be as high as 10^8. Thus, although χ_0 might easily be 10^{-11}, and hence the static magnetization $\chi_0 H_0 = 10^{-7}$ G, the dynamic susceptibility at resonance may be 10^{-4}. Of course, the probing field H_1 is necessarily small (to be discussed), but the magnetization is at ω_0 rather than zero frequency, so the relatively simple techniques of rf signal amplification and detection are used.

Had we not neglected the difference between M_0 and M_z in Eq. (2-39c), the algebra leading to Eq. (2-43) would have been more complicated, but far from intractable. The result would have been to add the term $\gamma^2 {H_1}^2 T_1 T_2$ to the denominator of Eqs. (2-43a) and (2-43b), so that (2-43b), for example, would read

$$\chi'' = \frac{\chi_0 \omega_0 T_2}{2} \frac{1}{1 + (\omega - \omega_0)^2 {T_2}^2 + \gamma^2 {H_1}^2 T_1 T_2} \qquad (2\text{-}44)$$

The term $S = \gamma^2 {H_1}^2 T_1 T_2$ is called the saturation factor. Regarded as a function of S, the absorbed power, $2{H_1}^2 \chi'' \omega_0$, is a maximum when $S = 1$. For $S \gg 1$, χ'' tends to zero; the resonance is said to be saturated.

The solution for M_z including saturation is also interesting:

$$M_z = \chi_0 H_0 \frac{1 + {T_2}^2(\omega_0 - \omega)^2}{1 + {T_2}^2(\omega_0 - \omega)^2 + \gamma^2 {H_1}^2 T_1 T_2} \qquad (2\text{-}45)$$

It is worth displaying (and worth the student's time obtaining), because it can be used with previous general remarks to calculate W_{rf}.

Recall Eq. (2-27) for the excess population n:

$$n = \frac{n_0}{1 + 2W_{rf}T_1} \tag{2-27}$$

Using $n_0\gamma\hbar = 2\chi_0 H_0$, and $M_z = \frac{1}{2}n\gamma\hbar$, we equate (2-27) and (2-45) to obtain

$$W_{rf} = \frac{1}{2}\frac{\gamma^2 H_1^2 T_2}{1 + T_2^2(\omega_0 - \omega)^2} \tag{2-46}$$

Note the rapid diminution of the transition probability as the rf frequency ω differs from ω_0. Of more interest is W_{rf} at $\omega = \omega_0$. To generalize as much as possible, we must consider the line shape for an absorption experiment. It is, of course, χ'', but we wish to express that shape as a function of $\nu = \omega/2\pi$, $g(\nu)$, which is normalized to unity:

$$\int_0^\infty g(\nu)\,d\nu = 1$$

The correct $g(\nu)$ for a Lorentz line is

$$g(\nu) = \frac{2T_2}{1 + 4\pi^2 T_2^2(\nu_0 - \nu)^2}$$

Value of $g(\nu)$ is $2T_2$ at $\nu = \nu_0$. Returning to Eq. (2-46), we then can substitute for T_2 the quantity $\frac{1}{2}g(\nu_0)$, and we get, for $\nu = \nu_0$,

$$W_{rf} = \tfrac{1}{4}\gamma^2 H_1^2 g(\nu_0) \tag{2-47}$$

This formula is, in fact, the quantum mechanical result (the "golden rule") for the transition probability of a spin $\frac{1}{2}$ system, where the quantity $g(\nu_0)$ is the "density of final states," which explicitly expresses the width of the level via the shape and normalization. The quantity $\gamma^2 H_1^2/4$ is obtained from the square of the matrix element of the perturbation $-\mu_x H_1$ between the initial and final states:

$$|\langle\tfrac{1}{2}|\gamma H_1 I_x|-\tfrac{1}{2}\rangle|^2$$

Finally, to complete our earlier discussions, we can equate (2-33), $P = 2H_1^2\chi''\omega$, and (2-28), $P = n_0\hbar\omega W_{rf}/[1 + 2W_{rf}T_1]$, and solve for χ'', which turns out to be (2-44). We conclude that the Bloch equations are consistent with our general discussions about energy absorption based on detailed balancing.

2-6. SOME EXPERIMENTAL CONSIDERATIONS

A great variety of experimental arrangements to observe nuclear magnetic resonance have been successfully used. Descriptions of some of the earlier ones are in the book by Andrew [4]. Although Andrew's book is old, most of the basic techniques still in use are described there. We want to analyze the experimental problem in a general way to establish the understanding with which the student can investigate on his own any particular circuit he may wish. Although our discussion will be couched in the language of radio frequencies—coils and capacitors are prominent—rather than microwave frequencies where resonant cavities are usually used, the analysis is really sufficiently general to apply to the microwave case also.

Q-meter detection

Consider a coil the inductance of which in the absence of a sample is L_0. If a sample of permeability μ occupies all space threaded by the magnetic lines of force generated by a current through the coil, then the inductance of the coil becomes

$$L = \mu L_0 = (1 + 4\pi\chi)L_0 \tag{2-48}$$

If the sample does not fill all space, the susceptibility χ must be multiplied by the filling factor η, as in Eq. (2-38). The quantity χ in Eq. (2-48) is the *complex* susceptibility defined in (2-31). Since no coil exists without resistance, unless it is made of superconducting wire, we must really always specify the coil's resistance R_0 as part of the coil. Our problem is to calculate the coil impedance $\mathscr{Z}_L = R_0 + i\omega\mathscr{L}$. Since $\mathscr{L}$ is complex, $i\omega\mathscr{L}$ has a real part (assume $\eta = 1$):

$$\mathscr{Z}_L = R_0 + i\omega[1 + 4\pi(\chi' - i\chi'')]L_0$$

$$= R_0 + 4\pi\omega L_0\chi'' + i[1 + 4\pi\chi']\omega L_0$$

To design an experimental method of detecting χ' and χ'', we must know their size relative to other terms in Eq. (2-49). Let us use, for numerical purposes, a fairly typical sample having a resonant frequency of 10 MHz in 10^4 G, and with a static susceptibility, χ, of 10^{-11}; $T_1 = T_2 = 10^{-3}$ sec. Then $4\pi\chi$ has a maximum value of 10^{-7}. A coil of wire that is useful at 10 MHz has an inductance of, say, a microhenry, so $\omega L_0 \simeq 60\ \Omega$, and a reasonable R_0 would be 1 Ω. Therefore, the reactive (imaginary) part of $\mathscr{Z}_L$ changes by one part in 10^7 as we go through resonance, and the resistive part changes by the fractional amount $4\pi\omega L_0\chi''/R_0 = 10^{-5}$. (It

is convenient to identify the ratio $\omega L_0/R_0 = Q$ as the "quality factor." See a text on ac circuits if you are unfamiliar with the definitions and uses of this parameter in resonant circuits.) We conclude that a necessary feature of any circuit design is that it be particularly sensitive to small changes in the real or imaginary part of $\mathscr{Z}_L$.

With few exceptions, the coil L is used in a resonant circuit by placing a capacity C_0 in parallel with L such that the Larmor frequency, γH_0, is the same as the resonant frequency $\omega_0 = 1/(L_0 C_0)^{1/2}$. The simplest conceivable circuit for observing a nuclear resonance is the so-called "Q-meter" circuit, shown in Fig. 2-6. The oscillator and large resistor R

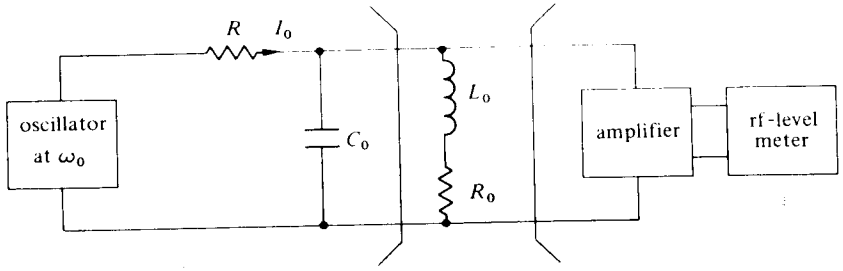

Fig. 2-6 Block diagram of Q-meter nuclear magnetic resonance detector.

form a constant current generator of current I_0. The parallel resonant circuit, tuned to ω_0, presents an impedance that, at resonance, is real: $Z_0 = Q\omega_0 L_0$. The voltage across it, $V_0 = I_0 Z_0$, is amplified, and its magnitude is detected by the peak-reading voltmeter. From Eq. (2-49), we see that as we go through resonance by changing H_0, for example, the real part of $\mathscr{Z}$ changes fractionally by the amount $4\pi\chi''Q$, so that the voltage at the amplifier input changes by

$$\Delta\mathscr{V} = I_0 4\pi\chi'' Q^2 \omega L_0$$

or by the fractional amount

$$\frac{\Delta\mathscr{V}}{V_0} = \frac{I_0 4\pi\chi'' Q^2 \omega L_0}{I_0 Q \omega L_0} = 4\pi\chi'' Q \tag{2-49}$$

We shall now give a word of explanation as to why we were able to ignore the change in reactance of the resonant circuit. For future uses it is best explained with a diagram, rather than analytically. Figure 2-7 is a complex plane diagram, sometimes called a "phasor" diagram, in which the magnitude and phase of the off resonance voltage across the sample is

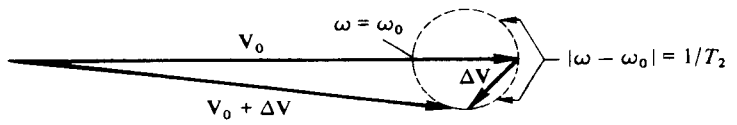

Fig. 2-7 Magnitude and relative phase diagram for voltages in Q-meter detection.

given by V_0, the "signal" voltage by $\Delta\mathscr{V}$, and the total voltage by $V_0 + \Delta\mathscr{V}$, the *magnitude* of which is detected by the peak-reading voltmeter. The complex signal $\Delta\mathscr{V}$ is given by

$$\Delta\mathscr{V} = -V_0(4\pi\chi'' + i4\pi\chi')Q \tag{2-50}$$

Reference to Eq. (2-50) and Fig. 2-7 shows that only the component of $\Delta\mathscr{V}$ in phase with V_0 is effective in determining the *length* of $V_0 + \Delta\mathscr{V}$. Since V_0 is real, because $Z_0 = Q\omega_0 L_0$ is real, the Q-meter circuit detects only χ'' to first order. The imaginary component, $-iV_0 Q4\pi\chi'$, is said to be in quadrature and affects the length only to second order in χ'.

The analysis of the "series-parallel" resonant circuit of Fig. 2-8a is

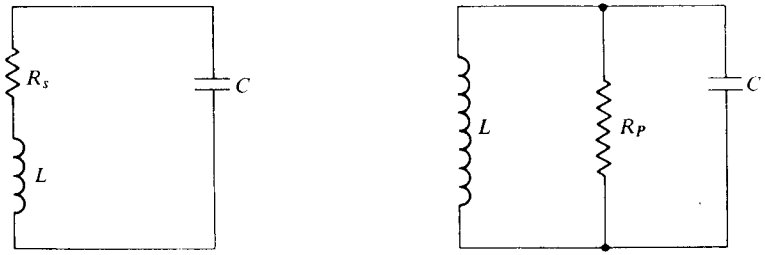

Fig. 2-8 (a) Series-parallel tank circuit. (b) Equivalent parallel circuit.

algebraically clumsy. Equation (2-50) is an approximation not only to first order in χ, but also to the extent that $\omega_0 = 1/(L_0 C_0)^{1/2}$ is the resonant frequency only in the approximation $Q \gg 1$. It is more convenient to analyze the *admittance* $\mathscr{Y}$ of the equivalent parallel circuit, Fig. 2-8b. The fictitious resistance R_P is related to R_s, in the high Q approximation, by $Q = \omega L/R_s = R_P/\omega L$. Then it is easy to show that $\mathscr{Y} = 1/R_P(1 + 4\pi\chi Q)$, and, by virtue of the smallness of χ, $\mathscr{Z} = 1/\mathscr{Y} = R_p(1 - 4\pi\chi Q)$, when $\omega_0 = 1/(L_0 C_0)^{1/2}$—hence Eq. (2-50).

The discussion of the "Q-meter" detector, so named because the

detected voltage is proportional to the change in Q of the circuit, hence to χ'', was phrased to make it clear that the working of the circuit depends on the *selection* of the component of the signal in phase with a much larger voltage, in this case V_0. A clear grasp of this concept is necessary to appreciate the operation of bridges in magnetic resonance detection.

Figure 2-7 and the subsequent discussion make the point that the Q-meter circuit picks out χ'' because V_0 and $4\pi Q\chi'' V_0 = \mathrm{Re}(\Delta\mathscr{V})$ are in phase. A large number of bridge circuits have been devised to accomplish this purpose, both in the microwave and rf regions. The archetype of the rf phase reference or coherent detection technique can be summarized in the block diagram of Fig. 2-9. In the discussion, it is understood that in

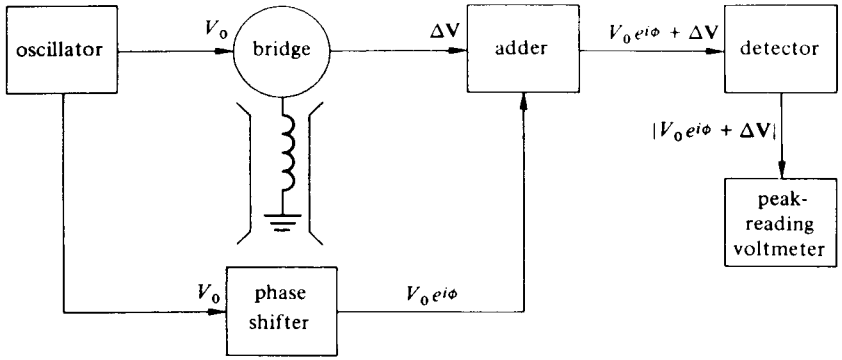

Fig. 2-9 Schematic archetypical bridge circuit.

the output of the oscillator $V_0 e^{i\omega t}$, the $e^{i\omega t}$ is suppressed. We assume V_0 is real for simplicity. The "bridge" is a device which, when balanced, has zero output, and which is unbalanced by the change in sample circuit impedance on resonance. The only output is the signal voltage $\Delta\mathscr{V}$. The phase shifter in Fig. 2-9 shifts the phase of the oscillator voltage by ϕ and supplies a reference signal to the adder, whose output is $V_0 e^{i\phi} + \Delta\mathscr{V}$. The detector is just the "peak-reading voltmeter" as before, and the amplitude $|V_0 e^{i\phi} + \Delta\mathscr{V}|$ is, to first order in $\Delta\mathscr{V}$, just V_0 plus the component of $\Delta\mathscr{V}$ in phase with the reference signal. One may write down the result more easily by pretending we shifted the phase of $\Delta\mathscr{V}$ by $(-\phi)$ instead of the phase of V_0 by $(+\phi)$ and by computing the real part of $\Delta\mathscr{V} e^{-i\phi}$:

$$\mathrm{Re}(\Delta\mathscr{V} e^{-i\phi}) = 4\pi V_0 Q\chi'' \cos\phi - 4\pi V_0 Q\chi' \sin\phi \qquad (2\text{-}51)$$

Choosing $\phi = 0$ with the phase shifter gives χ'', $\phi = 90°$ chooses χ', and, as advertised, any admixture may be chosen as well.

In real experimental arrangements, the functions of two or more of the separate components of Fig. 2-9 are usually combined into one device. If a real rf bridge is used in place of the box marked "bridge" in Fig. 2-9, it may be balanced by dividing V_0 and sending half of it through an arm, after which it recombines with the half that went through the signal arm with, of course, equal amplitude and opposite phase. If the bridge is operated in this fashion, completely balanced (off resonance, anyway), then the reference part of Fig. 2-9 is needed. Often, the bridge is unbalanced either in amplitude or phase (or a combination of the two), so that the steady unbalance signal is much larger than the signal. Then the external reference channel in Fig. 2-9 is unnecessary, and the unbalanced bridge has also performed the function of the adder. On the other hand, if the bridge is balanced, the "adder" and detector may be combined, as is often done in modern instrumentation, by using a device called a "mixer," which takes two signals applied to two inputs and puts out of the third port the sum and difference frequencies. In our case, the difference frequency is zero, and its magnitude is given by Eq. (2-51).

Every statement previously made for rf techniques (frequencies up to, say, 100 MHz) has its equivalent in microwave techniques. The tuned LRC circuit is replaced by a resonant cavity, which has a "Q" and to which the language of impedances, voltages, and currents may also be applied. Microwave bridges are in many ways easier to understand than the older rf circuits, and in recent years there has become available an rf version of the time-honored component of the microwave bridge, the hybrid junction or "magic tee." It is now possible to make a nuclear resonance spectrometer that is an exact copy of the microwave equivalent, even to the extent of the language used to describe it.

All the original nuclear resonance by the Harvard and Stanford groups used bridge techniques. The Stanford group lead by Bloch used a device, the crossed coil spectrometer, which is perhaps the instrument of choice if space around the sample permits. A sketch of the essentials of the arrangement is shown in Fig. 2-10. Unlike other methods the bridge balance is achieved by geometry. The field H_1 is applied in the y direction in the laboratory by the split coil called the transmitter coil, and the signal is induced in the orthogonal coil, the receiver coil, in the x direction of the laboratory frame. Remember that the induced magnetization rotates in the xy plane; thus either coil sees a magnetization varying at frequency ω. The bridge is balanced because, in principle, the lines of flux from the transmitter do not link any receiver coil turns. The unbalance is achieved by the natural lack of complete orthogonality, and control of the unbalance can also be achieved by mechanical means with "paddles," devices that "steer" the flux by means of currents induced in them by the field. Since the balance is achieved mechanically, it is somewhat broad band, and the

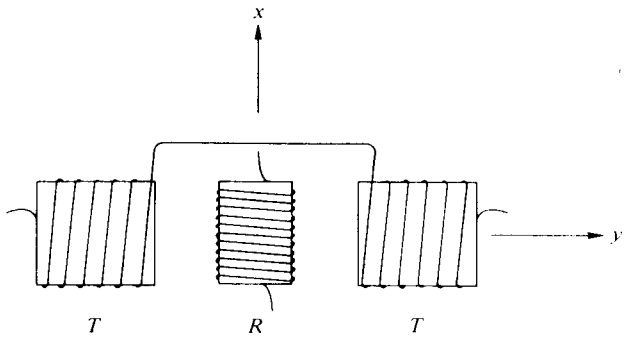

Fig. 2-10 Crossed coil geometry: T is the split transmitter coil and R the receiver coil containing the sample; H_0 is applied perpendicular to the page. Not shown are flux steering arrangements (paddles).

resonant frequencies of the transmitter and receiver can be swept synchronously if necessary. One can also balance as well as possible mechanically and achieve the rest of the balance and the reference through an electronic phase shifter, as in Fig. 2-9. There has even been a microwave version of the crossed coil spectrometer, with two resonant cavities coupled by the sample.

One somewhat academic difference exists between what is measured by the crossed coil apparatus and the others we have discussed. Strictly speaking, the complex susceptibility χ is a tensor rather than a scalar quantity, and the single coil measures the response M_x to a field applied in the x direction: we should write $M_x = \chi_{xx} H_{1x}$. The crossed coil apparatus measures χ_{xy}, since the receiver coil is in the x direction and the transmitter coil is in the y direction: $M_x = \chi_{xy} H_{1y}$. There is no case in pure nuclear magnetic resonance in which the distinction is important, since the precessing magnetization is circularly polarized. In the case of pure quadrupole resonance (see Chapter 4), the magnetization is actually linearly polarized, and $\chi_{xy} = 0$; the crossed coil technique does not work!

Marginal oscillators

Bridge and Q-meter circuits separate the function of oscillator and receiver. The separation of these functions has the advantage that the oscillator contribution to the noise of the device can be made negligible, so that the entire noise generation is in the receiver and sample circuits. The separation of these functions has the disadvantage that it is awkward to sweep the frequency rather than the external field in displaying the resonance or in searching for it. That objection is less true of the crossed

coil circuit, previously mentioned, because the bridge balance depends on geometry rather than on a number of frequency sensitive circuit elements. Still, it is quite awkward to sweep over a factor of three in frequency unless the generator and receiver functions are combined. That object is achieved if the sample tank circuit is made a part of the oscillator tank. The device is then operated so that the voltage level of oscillator depends critically on the tank circuit Q. Although the term $4\pi\chi' Q$ also affects the frequency of oscillation, normally only the level of operation is monitored, so the circuit detects χ''. The circuits thus used are at least a factor of two less sensitive than bridge circuits (because of the contribution of oscillator noise), and they become very poor at low rf levels, where the noise properties of the combined oscillator-receiver system become poor. But the convenience of being able to sweep frequency by adjusting only the capacitor in the tank circuit has made these circuits very popular. Robinson has described a clever combination of Q-meter and marginal oscillator circuits that seems to have all the advantages of Q-meter and marginal oscillator circuits, plus the ability to operate with very low rf levels (to 100 μV) on the sample coil (Robinson [5]).

Detection techniques

We have progressed gently in this chapter from elementary statistical mechanics increasingly toward experimental considerations. This is as it should be, since the numerical magnitudes of magnetization, the dynamical behavior of that magnetization as it interacts with the externally applied fields with the lattice, and with itself (T_2), all force onto the experimentalist the techniques he uses. To conclude this chapter, we examine some of the methods commonly used—and used not only in magnetic resonance—to display with greater clarity, with as much freedom from noise interference as possible, the magnetic resonance signal. A few words about noise in general will have to suffice to establish the motivation for the techniques used; for even a modest step beyond mere introduction to the theory and practice of noise on electronic signals, the student will have to consult a text on the subject (particularly recommended is the book by Robinson [5]).

In discussing the various nuclear resonance techniques, we have sloughed over a number of crucial points in the interest of moving the narrative along. Let us remedy the fault by a rhetorical question: What are the major sources of noise in typical magnetic resonance experiments? The answer is oscillator noise, source noise, receiver noise, detector noise, and microphonics. The marginal oscillator circuits are particularly susceptible to oscillator noise; the bridge circuits and Q-meter circuits may be operated so that oscillator noise is not a factor. Receiver noise is the

best kind to have limiting your experiment because it can be combatted by application of design skill and/or money, and it will always be a limitation until it is smaller than the inherent noise of the source. The detector, the device that converts the radiofrequency into direct current, has one important property. It is usually a diode, so it converts to direct current efficiently only when the radiofrequency applied to it is, say, greater than $\frac{1}{2}$ V. That is another rather good reason for applying a sizable reference radiofrequency in addition to the large one required by our analysis of phase detection.

Now, if the device labeled "peak-reading voltmeter" in Fig. 2-9 is actually a dc instrument, one is at the mercy of the instabilities of dc amplifiers, since very frequently rf amplification preceding detection is insufficient to provide a signal of convenient size. The problem is overcome by modulating the signal at an audiofrequency ν_m, so that the detected signal is at frequency ν_m, not zero, and may be amplified further. If the signal is somehow modulated, the detected signal is at ν_m and noise near ν_m is of importance. Diodes contribute noise with a $1/\nu$ frequency spectrum down to quite low frequencies. This restriction is particularly important for microwave diode detectors. Microphonic noise may, in principle, be overcome by good experimental design, but the ideal is often hard to achieve in practice. Those with long experience with microphonics seem to agree that a noise spectrum of $1/\nu$ may not be bad approximation in practice.

The source noise remains. A parallel tuned circuit on resonance looks like a resistance $R_s = Q\omega_0 L_0$. The unavoidable noise presented to the input terminals of the receiver is called Johnson noise, and is given by the Nyquist formula

$$V_N^2 = 4R_s k_B T \Delta\nu \tag{2-52}$$

where the noise resistance V_N is in volts, R_s is in ohms, T is in degrees Kelvin, k_B, Boltzmann's constant, is 1.38×10^{-23} J/K, and $\Delta\nu$, the bandwidth, is in sec^{-1}. Note that Eq. (2-52) depends on $\Delta\nu$, but is independent of ν, the center frequency.

Put together all these factors and one concludes that the game to play is to modulate the signal at as high a frequency as possible and to use as narrow a bandwidth as possible, dictated by Eq. (2-52). Figure 2-11 shows schematically the most common method for impressing a modulation on a signal. The ordinate is χ'' and the abscissa is H_0, which is varied around the mean value by an amount H_m, at frequency ν_m. Thus, $H(t) = H_0 + H_m \cos 2\pi\nu_m t$, say. If H_m is smaller than $1/\gamma T_2$, the rf signal at the detector will be $V(t) = (V_0 + V_m \cos \omega_m t) \cos \omega_0 t$, where V_m is proportional to $d\chi''/dH_0$. The last clause follows from Fig. 2-11, and would be

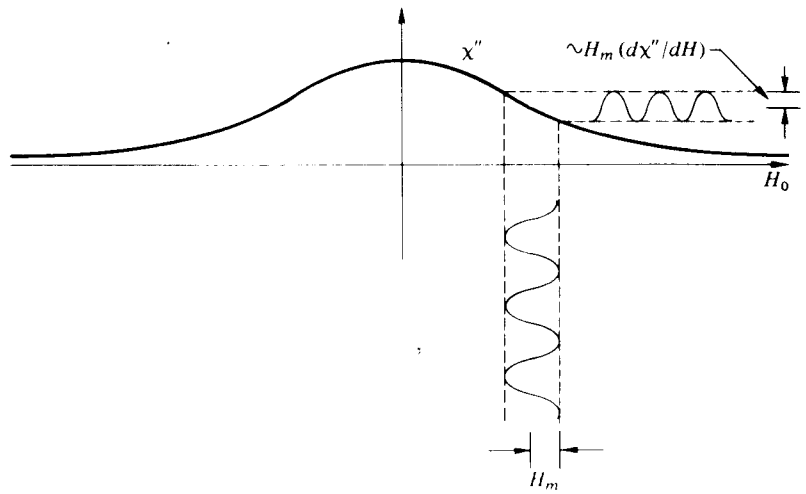

Fig. 2-11 Graph to show that lock-in detects $d\chi''/dH$.

exact if χ'' were exactly straight between $H_0 - H_m$ and $H_0 + H_m$: the output signal $V(t)$ is amplitude modulated with a modulation depth proportional to the derivative of χ'', at least to first order in an expansion parameter $\gamma T_2 H_m$. The frequency spectrum of the amplitude modulated rf signal has a main peak at ν_0 and sidebands at $\nu_0 \pm \nu_m$. The signal power is in the sidebands. After detection (now we had better say after the *first* detector), the signal power is at a frequency ν_m. ν_m is usually a low audio frequency for nuclear resonance, but may be as high as 100 kHz in some commerical electron spin resonance spectrometers. ν_m must satisfy the requirements $\nu_m \ll 1/T_2$, so that the magnetization can follow the field and always be in the steady state corresponding to our solutions of the Bloch equations.

The ultimate signal we wish to record is to be at direct current, that is, at $\omega = 0$. Clearly the job can be accomplished by the same method by which the rf signal was rectified, and, for much the same reasons, a phase-sensitive detector is employed. Since the phase of the audio signal carrying the signal power is known, phase-sensitive detection at the audio frequency may be used to discriminate against noise at ν_m not in phase with the signal at ν_m. The device that accomplishes this task, the second detector, is often called a lock-in. The terminology originated in radar work during World War II.

Finally, the bandwidth $\Delta\nu$ is normally limited not by the bandwidth of an rf amplifier at ν_0, or the audio amplifier at ν_m, but by an RC network arranged as a simple "integrator" at the output of the lock-in detector.

Figure 2-12 shows $d\chi''/dH_0$ of the ^{27}Al resonance in aluminum metal, taken with the bridge, rf amplifier, and modulation lock-in technique described in this chapter.

There are many circumstances in which the signal is strong enough that signal modulation is neither desirable nor even possible. The only thing to be done is to sweep through the resonance with the external field fairly rapidly, making sure the subsequent amplifiers and detectors have enough bandwidth to reproduce the signal faithfully. During this rapid sweep, it may easily turn out that dH_0/dt may be too large to be ignored in the Bloch equations. Their solution then becomes much more difficult than our steady state solution; some of the details were worked out in the first investigation by Bloch *et al.*, since their experiments were done that way. Figure 2-13 shows a proton resonance in water. A problem at chapter's end deals with some of the aspects of that signal.

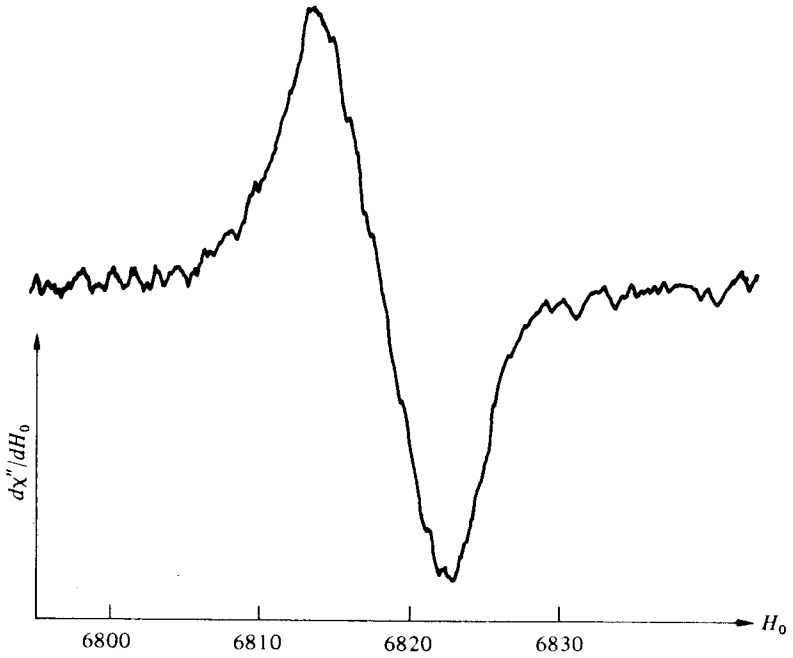

Fig. 2-12 Nuclear magnetic resonance signal, $d\chi''/dH$, of ^{27}Al in Al metal.

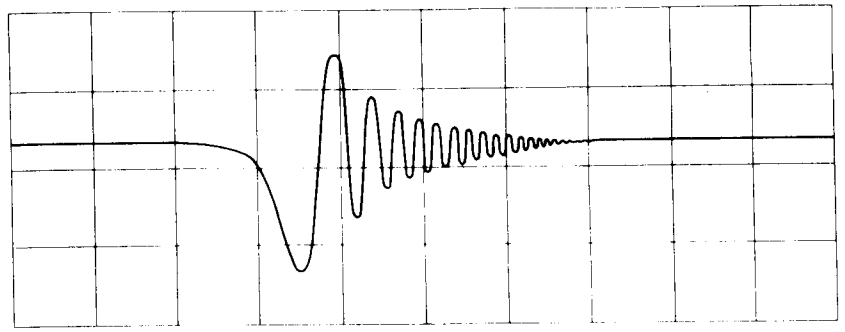

Fig. 2-13 Proton resonance in water, showing the phenomenon of "wiggles" (after Abragam [2], Figure III, 15).

Spin echoes

We conclude this chapter on some of the macroscopic aspects of magnetic resonance, and on the Bloch equations, by describing a phenomenon that appears, at first glance, to be too special, too clever a trick, to merit description in a text with an aim as general as ours. But the phenomenon of the spin echo, of a physical system emitting spontaneous signals if suitably prepared, has been exhibited in a sufficient variety of physical systems to make clear that it is a general property of systems with the sort of nonlinearity exhibited by the Bloch equations. The physical systems in which the spin echo has been seen, beyond the original nuclear magnetization system, include electron spin systems, atomic systems with induced electric dipole moments (at optical frequencies—the "photon echo"), and plasmas.

The spin echo is most easily seen in the following sort of system. Let T_2 and T_1 be rather long, but let T_2 be the parameter characterizing internal spin-spin interactions. Place the sample in a somewhat inhomogeneous external field $H_0 + H(r)$, so the variation of the external field over the sample, described by $H(r)$, can be described by a $T_0^* \ll T_2$. The coordinate r ranges over the sample. The following sequence of rf pulses is applied to the sample: (a) at $t = 0$, a 90° pulse; (b) at $t = \tau$, a 180° pulse, where $T_2 > \tau > T_2^*$. The result is a spontaneous signal of magnitude $V_0 \exp(-2\tau/T_2)$ appears at $t = 2\tau$.

Examine the process with the aid of Fig. 2-14. The 90° pulse tips M_0 into the x direction of the coordinate system rotating at $\omega_0 = \gamma H_0$ (see Fig. 2-14a). The "isochromats" precess in both directions relative to the x axis until they have fanned out completely, in $t \gtrsim T_2^* \simeq 1/\gamma\overline{H(r)}$, where $\overline{H(r)}$ is some average deviation of the field from H_0 (2-13b). Between the

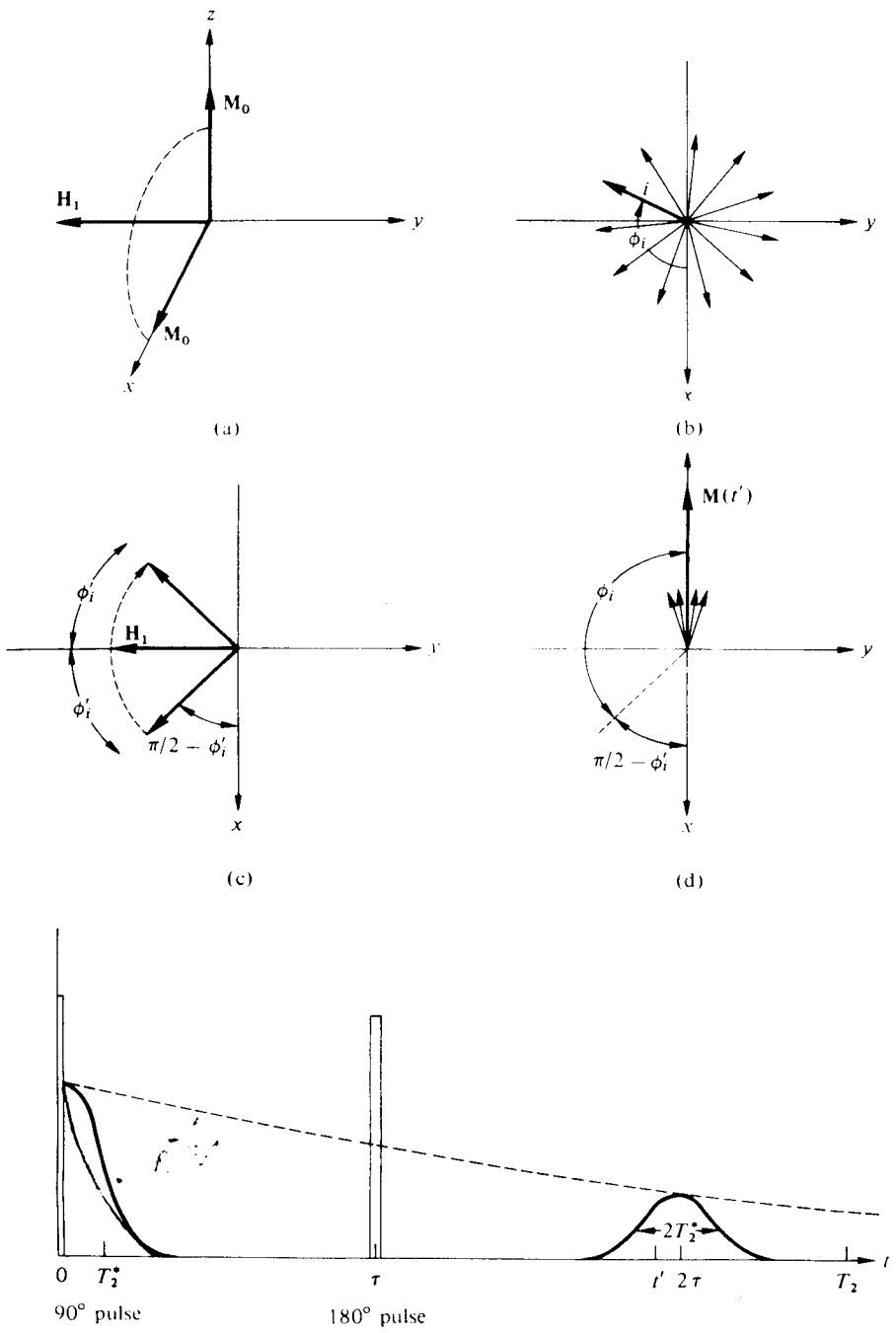

end of the 90° pulse and the beginning of the 180° pulse at $t = \tau$, a representative magnetization vector will precess relative to the x axis of the rotating frame by the angle $\phi_i = \gamma H(r_i)\tau$. The index i labels a particular small region of the sample. It is convenient to label the precession angle relative to the y axis: $\phi_i = (\pi/2) + \phi_i'$, where ϕ_i' is illustrated in Fig. 2-14b, for time t just before the 180° pulse. The 180° pulse flips the entire "pancake" about the y axis. The position of the magnetization that had precessed ϕ_i is shown in Fig. (2-14c). It is now at $\phi_i = (\pi/2) - \phi_i'$. It continues to precess in the same sense during the subsequent time, so that, at 2τ, it has accumulated another $\phi_i = (\pi/2) + \phi_i'$. The total phase accumulated at 2τ, including the 180° pulse, is thus $(\pi/2) - \phi_i' + (\pi/2) + \phi_i' = \pi$. The accumulated angle is independent of the labeling index i; therefore, all regions of the sample contribute to a signal at $t = 2\tau$, and all magnetization vectors add to form a macroscopic vector in the x direction in the rotating frame. The shape of the echo may be described as two free induction decays back-to-back, as shown in Fig. 2-14e. The signal is attenuated from the initial magnitude of the free induction decay, V_0, by *real* T_2 processes, which result in unrecoverable loss of phase coherence, as distinct from losses caused by static magnetic field inhomogeneities. If the echo height is measured as a function of τ, the 90° to 180° pulse separation, the echo height will follow the exponential $\exp(-2\tau/T_2)$.

The preceding example of a spin echo is the barest introduction. Many variations in pulse length, sequence, and number are possible. The technique is frequently used in the study of liquids and solids, where various contributions to the line widths can often be unraveled. There are many modern applications of the basic idea in seemingly remote fields, such as nonlinear optics and plasma diagnostics.

2-7. CONCLUSION AND LITERATURE SURVEY

Most of the material in this chapter is covered in every text and review article that discusses magnetic resonance. The material requiring statistical mechanics may be found in Feynman [6] and Reif [7], and, of course, all more advanced treatments of statistical mechanics. Treatments of the Bloch equations more or less on a somewhat more advanced level than found here are in the article by Pake [8], the books by Andrew [4], Kopfermann [9], Slichter [3], and Abragam [2]. Discussions of experimental

Fig. 2-14 (a) Effect of the 90° pulse on the magnetization vector $\mathbf{M}_0$. (b) "Pancake" formed in xy plane of rotating frame after $t > T_2^*$. (c) Effect of the 180° pulse on the ith magnetization vector. (d) Precessing magnetization vectors as echo is forming, corresponding to t' of (e). (e) Pulse sequence and signals seen at various times. t' corresponds to vector diagram of (d). Dotted line traces echo envelope as τ is varied.

techniques may be found in Andrew and Kopfermann. A totally exhaustive compendium of everything done until 1966 in the area of microwave instrumentation is in the book by Poole [10]. The previously mentioned monograph by Robinson [5] on noise in rf circuits gives an excellent and clear discussion of elementary principles, with applications in the last chapter to magnetic resonance instrumentation.

We should perhaps conclude by emphasizing that much of our discussion in this chapter is applicable beyond nuclear magnetic resonance, even though the language of NMR was used for convenience. The Bloch equations are not valid generally for nuclear or electron spins in solids (except conduction electrons in metals), but they are correct for liquids, and do serve to provide an introduction to the phenomena involved. It is also useful pedagogically to have them available for calculating χ' and χ'', in order to provide concrete examples of these important but slightly abstract functions. We remind the student that the chapter has been macroscopic—we moved as quickly as possible to macroscopic magnetizations and response functions for macroscopic samples. The "model theory" we used, the Bloch equations, was entirely phenomenological, and also dealt only with macroscopic magnetizations and fields. The observed signals are also macroscopic voltages, and the experimental problems of measuring them formed an important part of the chapter.

Problems

2-1. Find the correct approximation to Eq. (2-17) in the limit $\gamma\hbar H_0/2kT \ll 1$. What temperature T must be reached for protons ($\gamma = 2.6 \times 10^4$ G^{-1} sec^{-1}) in a field of 10^4 G before the high temperature approximation is wrong by 10%? Find the same quantity if the magnetic moment is that of the electron ($\gamma_e = 1.74 \times 10^7$ G^{-1} sec^{-1}).

2-2. Obtain Eq. (2-23) directly from Eq. (2-17) in the high temperature limit of problem 2-1. Find χ_0 for protons in water at room temperature.

2-3. From the Bloch equations and Eq. (2-33), obtain the maximum power absorbed per unit volume from the protons in water at 60 MHz. Use an H_1 that makes the saturation parameter $S = \gamma^2 H_1^2 T_1 T_2 = 1$ in Eq. (2-44). Assume $T_1 = T_2 = 3$ sec.

2-4. Find the approximate maximum voltage at the input of an rf receiver produced by the free induction decay after a 90° pulse applied to $Na^{23}Cl$. Assume a receiver coil of 5 turns, cross section 1 cm^2, and a resonant frequency of 10 MHz.

2-5. Find the signal at the receiver input from a spin echo in water under the following experimental conditions: coil, 10 turns, area 1 cm^2; pulses, 90 to 180° sequence, $\tau = 2$ sec, $T_2 = 3$ sec.

2-6. Invent other pulse sequences involving more than two pulses that give rise to other echoes. (There are almost limitless possibilities.)

2-7. Figure 2-13 shows the proton resonance in H_2O in a relatively homogeneous field. The beating phenomenon, known as "wiggles," arises because the external magnetic field is changing rapidly enough that the field is off resonance before the transverse magnetization has decayed. Since the magnetization precesses at a frequency proportional to the field, the signal beats with the constant oscillator frequency, and the constantly changing difference frequency appears in the detected signal as "wiggles." The sweep in Fig. 2-13 is linear at 0.1 sec and 5 mG per division. Estimate T_2^* from the figure and the field inhomogeneity at the sample.

2-8. The cw (continuous wave) or steady state resonance signal in a particular liquid sample consists of two nearby lines of equal intensity and transverse relaxation time T_2. Calculate the free induction decay following a 90° pulse if a transient experiment is performed. If the lines are separated by angular frequency $\Delta\omega$ in the cw experiment, show that an approximately 90° pulse can be applied to both with a single pulse applied at a frequency midway between the lines if the 90° pulse condition is satisfied, and the pulse length satisfies the inequality $\tau \ll (\Delta\omega)^{-1}$. (Satisfying the 90° pulse condition simultaneously means $H_1 \gg \Delta\omega/\gamma$, where $\Delta\omega/\gamma$ is the separation of the lines in field units. Such an H_1 is said to be sufficient to "cover" the lines.)

2-9. Discuss the shape of the echo formed after two pulses of problem 2-8.

References

1. G. Pake, *Paramagnetic Resonance*, W. A. Benjamin, Inc., New York (1962)
2. A. Abragam, *Principles of Nuclear Magnetism*, Oxford University Press London (1961).
3. C. P. Slichter, *Principles of Magnetic Resonance*, Harper & Row, New York (1963).
4. E. R. Andrew, *Nuclear Magnetic Resonance*, Cambridge University Press Cambridge, England (1955).
5. F. N. H. Robinson, *Noise in Electrical Circuits*, Oxford University Press London (1962).
6. R. P. Feynman, R. B. Leighton, and Matthew Sands, *The Feynman Lectures on Physics*, Addison-Wesley Publishing Co., Reading, Massachusetts vols. 1, 2, 3 (1965).
7. F. Reif, *Statistical Physics*, McGraw-Hill Book Company, New York (1967).
8. G. Pake, "Nuclear Magnetic Resonance," *Solid State Physics*, F. Seitz and D. Turnbull, Eds., Academic Press Inc., New York, vol. 2 (1956) pp. 1–91.
9. H. Kopfermann, *Nuclear Moments*, Academic Press Inc., New York (1958)
10. C. Poole, *Electron Spin Resonance; A Comprehensive Treatise on Experimental Techniques*, Interscience Publishers, New York (1967).

CHAPTER 3

Line Widths and Spin-Lattice Relaxation in the Presence of Motion of Spins

This chapter will be concerned with providing a microscopic model with which to estimate the parameters of the Bloch equations T_1 and T_2. To do so, we shall introduce the complementary concepts of random frequency modulation and random walk. The main use of these concepts will be to achieve a clear understanding of the motional narrowing of nuclear magnetic resonance lines, but the ideas are also important in the understanding of other experiments in modern physics, which we shall discuss in the latter part of the chapter.

3-1. INTRODUCTION

From a strictly economic point of view, magnetic resonance owes a great deal to its usefulness in chemistry. It is useful in chemistry because the nuclear magnetic resonance line widths in liquids are so narrow that resonant frequencies differing by as little as a part in 10^8 may often be resolved. It has been found that the frequency of nuclei in different chemical surroundings depends on the details of the surroundings. For example, the resonance frequencies of protons in ethyl alcohol, CH_3CH_2OH, are divided into three groups, corresponding to the protons in CH_3, in CH_2, and in OH. The *chemical shifts* caused by the different chemical environments are small, however, compared with the magnetic dipole-dipole interaction between the protons in the molecule, which corresponds to a magnetic field of 10 G produced on one proton by another an angstrom away. Our first guess ought to be that the resonance lines would be about 10 G wide, precluding a resolution of better than one part in 10^4. We shall be concerned with the solution to this apparent paradox in this chapter.

To complete and sharpen the paradox, we write down the magnetic field produced at a distance r by a point magnetic dipole.

$$\mathbf{H}_d = -\frac{\boldsymbol{\mu}}{r^3} + 3\frac{\boldsymbol{\mu}\cdot\mathbf{r}}{r^5}\mathbf{r} \tag{3-1}$$

The field $\mathbf{H}_d$ has the familiar dipole shape; the interaction energy of one dipole at the origin with another dipole at $\mathbf{r}$ has a rather complicated angular dependence, a $1/r^3$ radial dependence, and it depends as well on the relative orientation of the dipoles. Thus the dipolar field varies from site to site, and cannot be exactly the same for each nucleus. The simple estimate of $|\mathbf{H}_d| \simeq 10$ G between protons, for example, is calculated by using μ/r^3, where r is the nearest neighbor distance, and is to be taken as an estimate of the rough magnitude of local fields in hydrogenous solids. Thus we present the paradox as follows. The widths of nuclear resonance lines in a liquid can be a fraction of a cycle per second in the presence of local dipolar interactions as large as 50 kHz.

It is our purpose in this chapter to resolve the paradox both quantitatively and qualitatively, to discuss the Bloch equation relaxation times T_1 and T_2 as a function of the resonance field or frequency, and to broaden the discussion to include the phenomena of "exchange narrowing" and "exchange broadening" in nuclear and electron paramagnetic resonance, the Mössbauer effect, and the intensity of Bragg reflections in X-ray crystallography. We also hope to make clear the distinction between "motional narrowing" (a name for the effect we want to discuss) and the "pressure broadening" of lines in atomic spectra. It must be admitted at the outset that the way of understanding the phenomena that we shall develop is a natural one for magnetic resonance but not so natural for some of the other phenomena. Nevertheless, it is important to grasp phenomena from as many viewpoints as possible, so it is worth the strain placed on our method to do so.

The resolution of the paradox involves the recognition that in a liquid, a gas, and even in solids under some circumstances, the resonant spins can move substantial distances relative to their average spacing in T_2, and even in a Larmor period in some circumstances. Thus, the local fields with which we are dealing are not static but rather time dependent, most often in a random way, and we must develop ways to understand how the time dependence affects the resonance experiment. To begin with, we shall treat the problem temporally; that is, we shall examine the precession of a typical spin as a function of time. Although we shall thus provide ourselves with a useful formula with which we can estimate T_2 in a wide variety of cases, we shall not have grasped the significance of the term

"motional narrowing" until we have reexamined the problem in frequency space. To do that, we use some of the concepts and language of frequency modulation of a classical oscillator.

The language will be classical throughout, and we shall deal in qualitative estimates. Such an approach does the subject something of an injustice, since the phenomena are susceptible to quite precise and elegant formulation via the density matrix of quantum statistical mechanics. We henceforth banish from these pages any serious reference to the density matrix, and guide more ambitious and sophisticated readers to the text by Slichter [1].

3-2. RANDOM WALK CALCULATION OF T_2

We imagine ourselves sitting on a proton in water, for example, responding to the various magnetic fields in the sample. The strongest of these is the external field H_0, and we can dispose of it by looking at the world from a reference frame rotating at $\gamma H_0 = \omega_0$. The internal fields caused by the magnetic dipoles of other protons are random in orientation and time dependent. The z components of the local dipole fields add to or subtract from H_0 and cause a more rapid or less rapid precession than ω_0 about the z axis. In the rotating frame, these z components are responsible for the only existing precession about the z axis. Looking back at the discussion surrounding the Bloch equations in Chapter 2, the student should be able to recognize that these fields contribute to a T_2 process. We shall defer until later the discussion of T_1 processes, but it is appropriate here to identify their source. Precession of the spin *away* from the z axis is caused by transverse fields that are *static* in the rotating frame. Thus we expect local fields having components transverse to the z direction and frequency components at the Larmor frequency to contribute to T_1 processes. There is more to it than that, and we shall return to the T_1 problem later.

Let us construct a model of the longitudinal (z direction) local fields, and compute T_2. Let us presume that each spin in the sample sees a constant local field $h_L \ll H_0$ in the z direction for a time τ_c, after which it may or may not, with equal probability, reverse itself. In these terms, the problem can be phrased in terms of the famous "random walk" problem.[1] In that problem, the mean square distance traveled in the x direction, $\langle x^2 \rangle$, after n steps, each of length Λ in either the $+x$ or $-x$ direction, is

$$\langle x^2 \rangle = n\Lambda^2 \tag{3-2}$$

[1] For a derivation using arithmetical induction, see Feynman [2], vol. 1, p. 6–5.

In our problem, the unit of length is phase of precession about the z axis in the rotating frame, and the step length is $\gamma h_L \tau_c$. After time t, the number of steps n is t/τ_c; therefore, from Eq. (3-2), the mean square phase accumulated is

$$\langle \Phi(t)^2 \rangle = \frac{t}{\tau_c} (\gamma h_L \tau_c)^2 = \gamma^2 h_L^2 \tau_c t \tag{3-3}$$

It is perfectly within the spirit of the Bloch equations to identify T_2' as the time such that $\langle \Phi^2 \rangle = 1$ (rad)^2.[2] This criterion yields

$$\frac{1}{T_2'} = (\delta\omega)^2 \tau_c \tag{3-4}$$

where $\delta\omega = \gamma h_L$.

The particular problem we have "solved" seems a very artificial model for the behavior of internal fields in a liquid. The definitions of $\delta\omega$ and τ_c can be sharpened a great deal but at the expense of some mathematical complexity. As it stands, Eq. (3-4) provides an extremely useful estimate of T_2 in a liquid. If you wish to think of motions as being more "fluid," less jerky than the model suggests, then τ_c may be regarded as the time during which the local field changes by an amount comparable to its magnitude—a rather vague concept, to be sure, but one which might satisfy one's feeling that molecules are in continuous motion. Actually, the "jump" model has been shown by NMR techniques as well as by neutron diffraction to be a fair description of a liquid, in which a given environment around a given molecule persists for τ_c, followed by a change to another configuration, with the duration of the changing time being much less than τ_c. If one regards the constant τ_c to be an average, and the single local field to be an average over local fields caused by all possible local arrangements of nearly magnetic moments, then the picture may not look so unrealistic. And it should look quite good for describing the effect on the nuclear resonance line width of diffusion in solids.

Equation (3-4) is a reasonable estimate of T_2 as long as $\delta\omega\tau_c \gg 1$. If τ_c is long, the step length $\delta\omega$ is itself, when divided by γ, the width of the resonance line. So in the presence of a changing local environment, the line width is narrower than the static line width $\delta\omega$, as long as the local environment changes rapidly compared with $1/\delta\omega$.

Equation (3-4) is useful in a wider variety of circumstances than the student can presently imagine. We digress for a paragraph from the

[2] The use of the notation T_2' instead of T_2 will be explained later, when T_1 processes are discussed. The distinction between T_2 and T_2' is made here to indicate that we may not have included all possible sources of T_2 in this discussion.

main line of thought to show the application of measurements to the measurement of the diffusion constant. Let τ_c be the mean time between jumps or changes in the local environment. Imagine that a spin jumps spatially an interatomic distance a_0 each time. It proceeds, then, by random walk (in three dimensions) and travels in time t a mean square distance

$$\overline{l^2} \simeq \frac{t}{\tau_c} a_0 \tag{3-5}$$

The process described is called diffusion. It is described in continuum theory by a differential equation in the concentration c of the diffusing constituent:

$$D \nabla^2 c - \frac{\partial c}{\partial t} = 0 \tag{3-6}$$

The constant D is the diffusion coefficient. If Eq. (3-6) is solved for simple initial conditions and one-dimensional geometries, the root mean square distance the concentration spreads in time t from an initial concentration is approximately $(2Dt)^{1/2}$. Thus in Eq. (3-5) we identify

$$D \simeq \frac{{a_0}^2}{2\tau_c} \tag{3-7}$$

Since a_0 is related to the density, we have in Eq. (3-7) an expression for τ_c in terms of macroscopic quantities that can be determined by quite different, nonresonance experiments. Alternatively, we see from Eq. (3-4) that T_2 measurements can provide a value for the diffusion constant D, a number frequently hard to get if one is concerned with the self-diffusion of a molecule surrounded by identical molecules—H_2O in H_2O, for example.

To summarize Eq. (3-4) and some of the subsequent discussion, we plot $\log T_2$ versus τ_c in Fig. 3-1. The abscissa might easily be $1/D$ or η/T, where η is the viscosity and T the absolute temperature. For justification of the last clause, see the reprint of Bloembergen's thesis [3], the original work in the field. Note in Fig. 3-1 the leveling off of T_2 to $\delta\omega^{-1}$ at a value of τ_c on the order of $\delta\omega^{-1}$, something we have justified only by a plausibility argument so far.

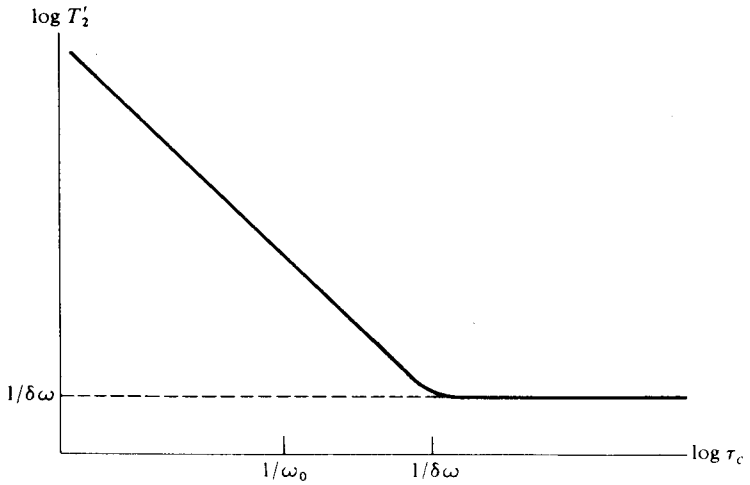

Fig. 3-1 Log T_2 versus log τ_c. Plot of Eq. (3-4) in region of its validity, $\delta\omega\tau_c < 1$.

3-3. VERY SHORT CORRELATION TIMES: $\omega_0 \tau_c \ll 1$

Suppose $\omega_0 \tau_c \ll 1$, and suppose the medium is spatially isotropic in the sense that the fluctuating internal fields point in no preferred direction. Then the magnitudes of the fields parallel to and transverse to H_0 are the same, and their frequency properties are also the same. As a result, the random walk in the transverse plane in the rotating coordinate system, produced as described in the last section, also occurs *away* from the z axis. This longitudinal relaxation, a T_1 process, is produced by transverse local fields *stationary* in the rotating frame, that is, at ω_0. The two independent and orthogonal random walks occur at *exactly the same rate* if the magnitude of the fluctuating fields at or near zero frequency is the same as at the Larmor frequency, ω_0. The simplest and most plausible description of the random internal field has that property if $\omega_0\tau_c \ll 1$.

Since there are two orthogonal transverse components of the local field in the rotating frame, and since they act independently, the mean square angular migration of a spin *away* from the z direction is

$$\langle \phi_{T_1}(t)^2 \rangle = 2\gamma^2 {h_L}^2 \tau_c t \tag{3-8}$$

just twice as great as in Eq. (3-3). Again setting $\phi_{T_1}(T_1)^2 = 1$, we obtain

$$\frac{1}{T_1} = 2(\delta\omega)^2\tau_c = \frac{2}{T_2'} \tag{3-9}$$

At this point, we see the reason for the introduction of the notation T_2' before Eq. (3-4). If we wish to calculate the parameter T_2, which characterizes the line width of a Lorentz line, we must include not only the inhomogeneity of the quasistatic local fields (so-called *secular* broadening), but also lifetime, or *nonsecular* broadening. Reexamination of the Bloch equation for M_x and a little thought produces the following conclusion. A T_2 process is one that causes precession of M_x away from the x axis of the rotating frame. Quasistatic fields in the z direction do this, as do fields in the y direction at ω_0. Fields in the x direction produce no effect because they exert no torque on M_x. Hence, we should have

$$\frac{1}{T_2} = \frac{1}{T_2'} + \frac{1}{2T_1} \tag{3-10}$$

where the first term is from Eq. (3-4) and the second is half of Eq. (3-9). Comparing Eqs. (3-4), (3-9), and (3-10), we see that

$$T_1 = T_2 \tag{3-11}$$

The equality holds in the limit $\omega_0 \tau_c \ll 1$ and depends, we reiterate, on spatial isotropy of the local fields. We have also filled in more of Fig. 3-1 if we regard it as a plot of T_2^{-1} or T_1^{-1} versus τ_c, rather than $(T_2')^{-1}$ versus τ_c; namely, the T_2 and T_1 curves for $\tau_c \ll 1/\omega_0$ coincide. To fill in the T_1 curve for longer τ_c we require more general analytical tools, the development of which we shall indicate in the next section.

3-4. RANDOM FREQUENCY MODULATION; SPECTRAL DENSITY

In this section we shall make heavy use of the analogy between a magnetic moment precessing at the frequency $\nu = (\gamma/2\pi)[H_0 + h_L(t)]$ and a classical, frequency modulated oscillator transmitting, for example, classical music at a center frequency of 97.8 MHz.

We shall begin by considering a proper mathematical description of frequency modulation. The simplest situation to treat is a sinusoidal frequency deviation; that is, the angular frequency of the oscillator is given by

$$\omega(t) = \omega_0 + \Delta\omega \cos qt \tag{3-12}$$

where $\Delta\omega$ is the frequency deviation and q is the frequency of modulation. We now need an expression for $A(t)$, the amplitude of the fm oscillator as a function of time. One approach might be to write

$$A(t) = A_0[\cos \omega(t)t]$$

We shall not number that equation, since it is wrong, just as it is wrong to write that the distance a car travels in t to be $d = vt$ if v is not a constant. The argument of a trigonometric function is a *phase*, and the phase accumulated between $t' = 0$ and t with frequency given by Eq. (3-12) is

$$\phi(t) = \int_0^t \omega(t')\,dt' = \omega_0 t + \frac{\Delta\omega}{q} \sin qt \tag{3-13}$$

Now we can safely write, complete with equation number,

$$A(t) = A_0 \cos\left[\omega_0 t + \frac{\Delta\omega}{q} \sin qt\right] \tag{3-14}$$

The ratio $\Delta\omega/q$ is an extremely important parameter for future discussions:

$$m = \frac{\Delta\omega}{q} \tag{3-15}$$

where m is called the *modulation index*. Its size relative to unity will be crucial in many applications.

We wish to know the frequency spectrum of Eq. (3-14). First, it is more convenient to rewrite Eq. (3-14) using the trigonometric identity $\cos(a + b) = \cos a \cos b - \sin a \sin b$:

$$A(t) = A_0[\cos \omega_0 t \cos(m \sin qt) \quad \sin \omega_0 t \sin(m \sin qt)] \tag{3-16}$$

From immediate inspection we can see that the main frequency components are at ω_0, and the other spectral content is caused by the terms $\cos(m \sin qt)$ and $\sin(m \sin qt)$. They are periodic with period $2\pi/q$; that is, the argument of these terms repeats itself with that period. That fact makes them prime candidates for expansion in Fourier series. Consider the cosine function

$$\cos(m \sin qt) = \sum_{n=0}^{\infty} a_n(m) \cos nqt \tag{3-17}$$

We can use only cosine terms in the expansion since the cosine is an even function and the coefficients of sine terms would necessarily vanish. The coefficients $a_n(m)$ are found by multiplying both sides of Eq. (3-17) by $\cos n'qt$ and averaging over a period T. If you do so, you find the following integral expression:

$$a_{n'}(m) = \frac{1}{T} \int_0^T \cos n'qt \cos(m \sin qt)$$

This expression may be developed in a power series in $m \sin qt$, which becomes, upon integration, a power series in m. Fortunately, the labor has already been done; consultation of a complete set of mathematical tables [4] under "Bessel Functions" shows the coefficients of Eq. (3-17) to be Bessel functions of integral order:

$$\cos(m \sin qt) = J_0(m) + 2\sum_{k=1}^{\infty} J_{2k}(m) \cos 2kqt \qquad (3\text{-}18a)$$

and

$$\sin(m \sin qt) = 2\sum_{k=0}^{\infty} J_{2k+1}(m) \sin[(2k+1)qt] \qquad (3\text{-}18b)$$

The functions $J_n(m)$ are Bessel functions of integral order of the first kind. Although they are surely less familiar than trigonometric functions, the student should not be put off by them. A graph of the first three is shown in Fig. 3-2. Note $J_0(0) = 1$, and $J_n(0) = 0$, $n = 0$. Also note that $J_0(m)$ deviates as m^2 from its value at $m = 0$ for small m, and the others begin from zero as m^n. A qualitative look at Fig. 3-2 and these remarks are all we require of the Bessel functions. The expressions (3-18) must be put back into (3-16):

$$A(t) = J_0(m) \cos \omega_0 t + \sum_{n=-\infty}^{\infty} J_{|n|} \cos(\omega_0 + nq)t(\operatorname{sgn} n) \qquad (3\text{-}19)$$

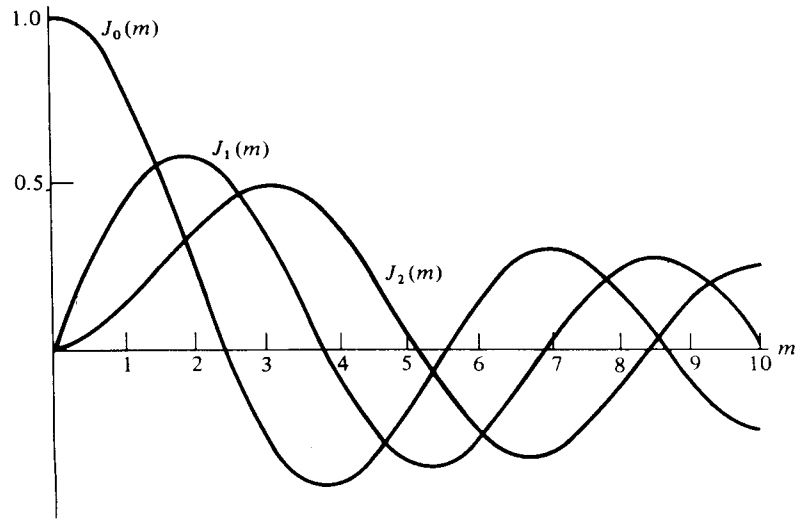

Fig. 3-2 Bessel functions of the first kind, $J_n(m)$, versus m, for $n = 0, 1, 2$.

The notation (sgn n) means to multiply by $(+1)$ when $n > 0$ and by (-1) when $n < 0$. Again, Eq. (3-19) is most valuable to use in graphical form, as in Fig. 3-3, which gives the frequency spectrum of the power, proportional to $A(t)^2$. The graph has been presented with $\Delta\omega$ = constant, because in our applications, the local field, which causes $\Delta\omega$, is a fixed characteristic of the substance, whereas q may often be changed within a given sample, by changing the temperature, for example. (We shall present one situation, however, in which it is q that is fixed by the nature of the substance and $\Delta\omega$ that is changed by the experimenter.) The thing to notice about Fig. 3-3 is that the power spectrum is mostly contained within $\Delta\omega$ of ω_0, and when $m < 1$, which means $q > \Delta\omega$, the power is mainly in the center frequency ω_0. The sidebands are still spaced by the modulation frequency q but are small in amplitude. If you try to change the frequency back and forth too rapidly, the major effect is not to change it at all.

Although there is only a qualitative resemblance between the problem of sinusoidal frequency modulation and our problem of motional narrowing, the results of the preceding analysis are already suggestive. If we make an arbitrary connection between the spectrum of Fig. 3-3 and the line width in a nuclear resonance, we can see the origins of the broadening that takes place as τ_c increases and becomes on the order of $1/\delta\omega$ in Fig. 3-1. For all values of τ_c such that $\delta\omega\tau_c < 1$, the "modulation index" is less than 1; that is, $\delta\omega\tau_c$ is roughly the same as the modulation index.

There is, of course, a vast difference between the case of sinusoidal modulation and the random fluctuations of the local field in a liquid. To

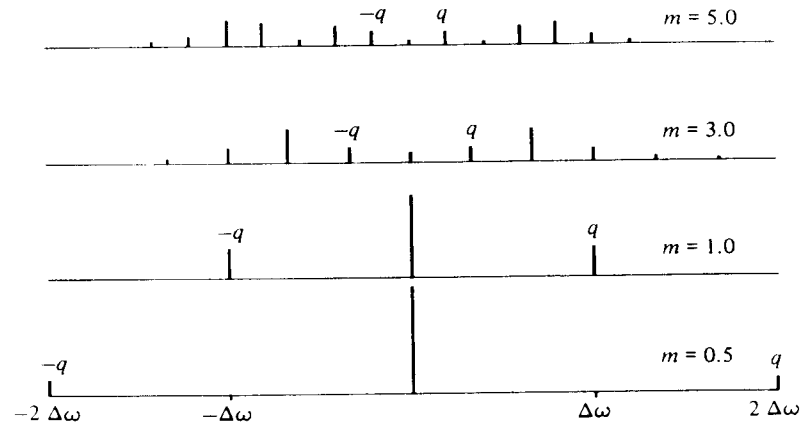

Fig. 3-3 Fourier components of the power spectrum of Eq. (3-19) for $m = 0.5, 1.0, 3.0, 5.0$.

sharpen the distinction, we make the following analysis. Let $h_L(t)$ be the local field seen by a nucleus at some arbitrary time t. Form the product $h_L(t)h_L(t+\tau)$ and average over all time for a particular nucleus. That process defines $f(\tau)$:

$$f(\tau) = \langle h_L(t)h_L(t+\tau)\rangle \tag{3-20}$$

where the brackets $\langle\ \rangle$ indicate average over time t and $f(\tau)$ is the *autocorrelation function* of h_L. It is independent of t since the sample is assumed to be homogeneous and in thermal equilibrium; there is nothing special about any particular time. Consider what we expect of $f(\tau)$ as τ becomes large. If the sample is large, if the local field is produced by many nuclei undergoing random motions, then we ought reasonably to expect no relation between $h_L(t)$ and $h_L(t+\tau)$. Since h_L can be positive or negative, and since, in fact, the temporal randomness of h_L means $\langle h_L(t)\rangle = 0$, we expect

$$\lim_{\tau\to\infty} f(\tau) = 0 \tag{3-21}$$

to be reasonable behavior for $f(\tau)$ at large τ. Contrast that behavior with the autocorrelation function of Eq. (3-12):

$$\begin{aligned}\langle\omega(t)\omega(t+\tau)\rangle &= \langle(\omega_0 + \Delta\omega\cos qt)[\omega_0 + \Delta\omega\cos q(t+\tau)]\rangle \\ &= \omega_0{}^2 + \Delta\omega^2\left(\frac{q}{2\pi}\int_0^{2\pi/q}\cos qt\cos q(t+\tau)\,dt\right) \\ &= \omega_0{}^2 + \Delta\omega^2\frac{\cos q\tau}{2}\end{aligned} \tag{3-22}$$

The leading term, $\omega_0{}^2$, is as expected, but the second term certainly does not vanish. Therefore, it is clear that a simple modulation such as Eq. (3-12) fails to satisfy one's intuitive requirements for random modulation.

The simplest form of $f(\tau)$ that satisfies all the requirements is an exponential:

$$f(\tau) = \langle h_L(t)^2\rangle \exp -|\tau|/\tau_c \tag{3-23}$$

Equation (3-23) reintroduces the correlation time τ_c. The average over time of the square of the local field, $\langle h_L(t)^2\rangle$, is the same as the average of $h_L{}^2$ over all the nuclei in the sample by a fundamental hypothesis of

statistical mechanics [5]. We see that we are able to specify the local field, and hence the random frequency modulation of each "nuclear oscillator" by that local field, less precisely than we did in the simple case of sinusoidal modulation, but we do preserve some points of similarity. These include the correspondence between $(\gamma h_L)^2$ and $\Delta\omega^2$, and the similarity between the parameter q of Eq. (3-22) and $1/\tau_c$ of Eq. (3-23).

At this point, our resort to plausibility arguments must come to an end, because the subsequent development relies on theory that uses the density matrix of quantum statistical mechanics and time dependent perturbation theory. The full theory is nothing less than a derivation of the Bloch equations from the basic principles of quantum statistical mechanics. Our previous paragraphs have attempted to establish a climate of acceptance in the student's mind for the results. The central formula of the theory is the Fourier transform of the correlation function $f(\tau)$, which is $j(\omega)$, the spectral density function:

$$j(\omega) = \tfrac{1}{2}\int_{-\infty}^{\infty}\langle h_L(t)h_L(t+\tau)\rangle e^{-i\omega\tau}\,d\tau \tag{3-24}$$

Equation (3-24) is one of a pair of integrals known as the Wiener–Khintchine relations (see reference [5], p. 586). In the case of the particular form of $f(\tau)$ given by Eq. (3-24),

$$j(\omega) = \frac{\langle h_L{}^2\rangle\tau_c}{1+\omega^2\tau_c{}^2} \tag{3-25}$$

The spectral density function determines the effectiveness of the local field in producing transitions between quantum mechanical spin states. The relaxation rates $1/T_1$ and $1/T_2$ are determined by $j(\omega)$. To write down the final results, we must specify $j(\omega)$ more completely. Since the local field has the usual x, y, and z components, a more general $j(\omega)$ may be written

$$j_{\alpha\beta}(\omega) = \tfrac{1}{2}\int_{-\infty}^{\infty} h_\alpha(t)h_\beta(t+\tau)e^{-i\omega\tau}\,d\tau \tag{3-26}$$

where $\alpha, \beta = x, y, z$. If the local field is truly random, then $\langle h_\alpha(t)h_\beta(t+\tau)\rangle = 0$, for $\alpha \neq \beta$, and the only components of $j_{\alpha\beta}$ are $j_{xx}(\omega)$, $j_{yy}(\omega)$, and $j_{zz}(\omega)$. In terms of the spectral density function, the complete equation for T_2^{-1} that replaces Eqs. (3-4) and (3-10) is

$$T_2^{-1} = \gamma^2[j_{zz}(0) + j_{yy}(\omega_0)] \tag{3-27}$$

The first term is the same as Eq. (3-4), which we obtained by the random walk argument, and the second is the "lifetime broadening" effect we discussed prior to Eq. (3-10). In terms of h and τ_c, from Eq. (3-25) we get

$$T_2^{-1} = \gamma^2\left(\langle h_z^2\rangle\tau_c + \langle h_y^2\rangle \frac{\tau_c}{1+\omega_0^2\tau_c^2}\right) \tag{3-28}$$

The assumption of spatial isotropy, made to obtain Eq. (3-10), is that $\langle h_x^2\rangle = \langle h_y^2\rangle = \langle h_z^2\rangle \equiv h_L^2$. The result for T_1^{-1} is

$$T_1^{-1} = \gamma^2[j_{xx}(\omega_0) + j_{yy}(\omega_0)] = \frac{2\gamma^2 h_L^2\tau_c}{1+\omega_0^2\tau_c^2} \tag{3-29}$$

We can now complete Fig. 3-1 by including the portion of the T_1 curve for $\tau_c > 1/\omega_0$. The full curve is shown in Fig. 3-4. At $\tau_c = 1/\omega_0$, T_1 goes through a minimum, then increases, whereas T_2 continues to decrease. Although these features are an obvious analytical consequence of

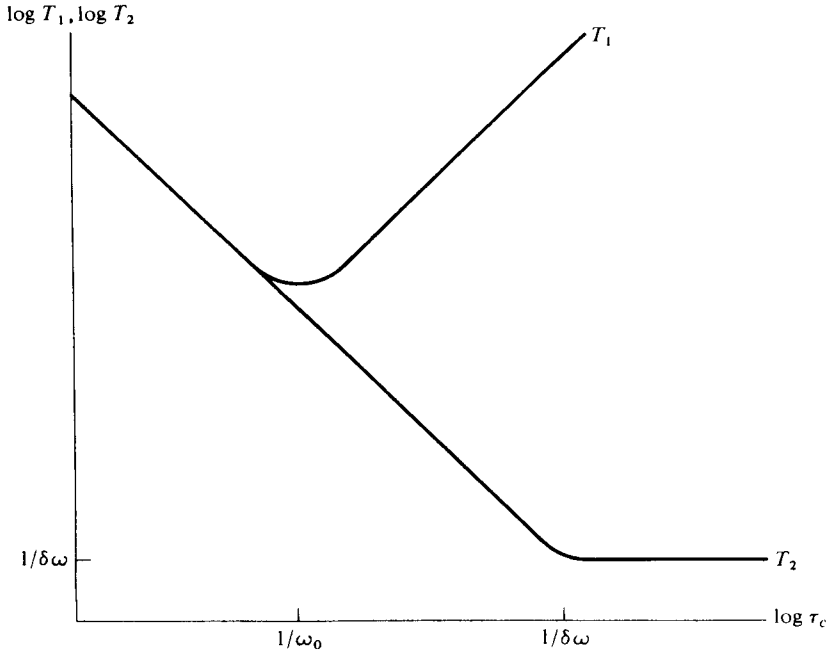

Fig. 3-4 Log T_1, log T_2 versus log τ_c for Eqs. (3-28), (3-29).

Eqs. (3-28) and (3-29), it is instructive to see how they can be remembered easily by examining one further property of $j(\omega)$, Eq. (3-25):

$$\frac{1}{h_L^2}\int_0^\infty j(\omega)\,d\omega = \int_0^\infty \frac{\tau_c d\omega}{1+\omega^2\tau_c^2} = \int_0^\infty \frac{dx}{1+x^2} = \frac{\pi}{2} \tag{3-30}$$

The area under $j(\omega)$ versus ω is a constant, independent of τ_c. Several $j(\omega)$ curves with this property are plotted in Fig. 3-5. When τ_c is short [curve (1) of Fig. 3-5], $j(\omega_0) = j(0)$, and $T_1 = T_2$. $j(\omega_0)$ is largest for curve (2)—hence the maximum in the relaxation rate there, or the T_1 minimum of Fig. 3-4. For long τ_c, $j(\omega_0)$ decreases again as the Larmor frequency falls far out in the tail of $j(\omega)$, accounting for the rise in T_1 for longer τ_c.

Nothing in Eq. (3-28) explains the constancy of T_2 when τ_c is longer than $1/\gamma h_L$. At this point, the theory breaks down, but the reason for it and the result can be seen in Fig. 3-3. The spectrum for $m \gg 1$ covers only the range $\Delta\omega$ as the modulation index increases. The local field is essentially static. Under these conditions, the Bloch equations are not valid, the line shape of the resonance, $\chi''(\omega)$, is not Lorentzian. We shall leave this case to the next chapter.

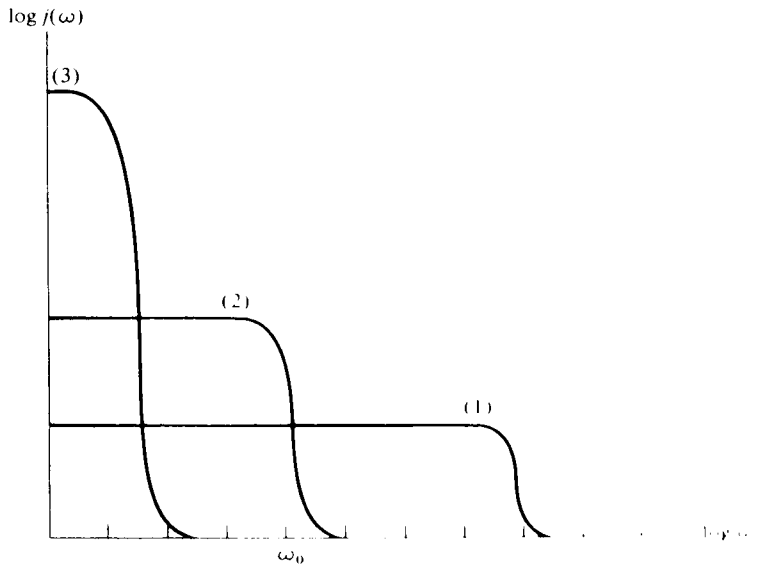

Fig. 3-5 (1) $j(\omega)$ versus ω, τ_c less than ω_0. (2) τ_c equal to ω_0. (3) τ_c greater than ω_0.

3-5. SOME APPLICATIONS

Qualitatively, the effect of rapid nuclear motion is to average out internal fields, or so the previous parts of this chapter would lead us to believe. In fact, we must be very careful to make a distinction between internal fields that can be averaged out and those that cannot. Equation (3-1) gives the expression for the field at a vector distance $\mathbf{r}$ from a point dipole

$$\mathbf{H}_d = -\frac{\boldsymbol{\mu}}{r^3} + 3\frac{\boldsymbol{\mu}\cdot\mathbf{r}}{r^5}\mathbf{r} \tag{3-1}$$

Consider, for example, the z component of the field produced at the center of a unit sphere by a dipole on the surface. If the dipole points in the z direction, then

$$H_z = -\mu(1 - 3\cos^2\theta)r^{-3}$$

where θ is the polar angle in the conventional spherical coordinate labeling. If the dipole is allowed to roam over the surface of the sphere, the average field at the center is

$$\frac{1}{4\pi}\int_{\phi=0}^{2\pi} d\phi \int_{\theta=0}^{\pi} (1 - 3\cos^2\theta)\sin\theta\, d\theta = 0$$

since $\langle\cos^2\theta\rangle = \frac{1}{3}$ when averaged over the solid angle. The demonstration of the equivalent result for other components of $\mathbf{H}_d$ and arbitrary orientation of $\boldsymbol{\mu}$ is tedious, and, in fact, unnecessary, but the result still holds.

Another type of *local* field that can be reduced by rapid motion is the inhomogeneity of the magnet. In this case, the inhomogeniety of H_z is all that counts. Suppose, as is likely to be the case in the typical electromagnet, the inhomogeneity has cylindrical symmetry, and suppose the maximum deviation from the average H_0 is ΔH. If a given nucleus can be forced to sample the range of fields over the sample volume rapidly enough, the total effect of the local field will be reduced according to Eq. (3-4). The nuclei may be caused to sample the magnet's range of fields by spinning the sample about an axis perpendicular to the field direction. A typical geometry is shown in Fig. 3-6. To achieve narrowing, ω must be so large that the modulation index, $m = (\gamma\,\Delta H/\omega)$, is less than one. If each spin samples essentially the same magnetic fields during each revolution, the frequency modulation produced by the spinning is periodic, although probably not sinusoidal. Our original analysis of frequency modulation is useful, though, and we see that the criterion $m < 1$ is sufficient to produce *spinning sidebands* which are farther away

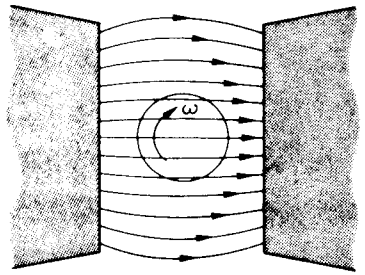

Fig. 3-6 Spherical sample in an inhomogeneous field. Sample is spun at angular frequency ω about an axis perpendicular to the page.

than $\gamma\,\Delta H$. For a typical field inhomogeneity of 10^{-4} G, such as is found in electromagnets made for chemistry applications, a spinning frequency $(\omega/2\pi)$ of a few cycles per second is sufficient. If turbulence within the sample causes a given spin to sample the available fields in a more random fashion, we require the width produced by the field inhomogeneity after narrowing to be comparable to, or less than, the natural width. The requirement from Eq. (3-9) may be expressed

$$\frac{1}{T_2} < \frac{1}{T_2^*} = \frac{(\gamma\,\Delta H)^2}{\omega} \tag{3-31}$$

For typical hydrogenous liquids, where $T_2 \simeq 5$ sec, and with a magnet inhomogeneity of 10^{-4} G, ω again must be a few cycles per second. That spinning rate is easily achieved, and commercial apparatus is routinely supplied with sample spinning attachments.